Titre: Title:	Stretchable Electrodes Using Conductive Polymers for the Detection of Vital Signs in Premature Infants
Auteur: Author:	Pierre Kateb
Date:	2023
Type:	Mémoire ou thèse / Dissertation or Thesis
Référence: Citation:	Kateb, P. (2023). Stretchable Electrodes Using Conductive Polymers for the Detection of Vital Signs in Premature Infants [Mémoire de maîtrise, Polytechnique Montréal]. PolyPublie. https://publications.polymtl.ca/55744/

POLYTECHNIQUE MONTRÉAL

affiliée à l'Université de Montréal

Stretchable electrodes using conductive polymers for the detection of vital signs in premature infants

PIERRE KATEB

Institut de génie biomédical

Mémoire présenté en vue de l'obtention du diplôme de *Maîtrise ès sciences appliquées*

Génie biomédical

Août 2023

POLYTECHNIQUE MONTRÉAL

affiliée à l'Université de Montréal

Ce mémoire intitulé :

Stretchable electrodes using conductive polymers for the detection of vital signs in premature infants

présenté par **Pierre KATEB**

en vue de l'obtention du diplôme de *Maîtrise ès sciences appliquées*

a été dûment accepté par le jury d'examen constitué de :

Rodney O'CONNOR, président
Fabio CICOIRA, membre et directeur de recherche
Gregory LODYGENSKY, membre et codirecteur de recherche
Veronika MAGDANZ, membre

DEDICATION

To the 120,000 forgotten hostages in Nagorno-Karabakh

ACKNOWLEDGEMENTS

I would like to start by thanking my supervisor Professor Fabio Cicoira to whom I am deeply grateful for offering the opportunity to work in his laboratory. His guidance and mentorship have shaped my academic journey.

I extend my gratitude to Dr. Gregory Lodygensky, my co-director, for his support, and invaluable expertise and insight on the needs of premature infants.

To all the members of our research group - Jiaxin, Gayaneh, Xin, Jeeyeon, Jinsil, Mona, Mina, Sadaf, Chi-hyeong, Jo'Elen, Meijing, Sara, Floriane, Claudine, Yang, Arun, Michel, Michael, Kathel, Erwan, Cécile, Noémy, Émily, Biporjoy, Yiting, Harini, Sally, Fumito, Hirofumi, Remi and Kate – My heartfelt thanks for their support, suggestions, and friendship. I have enjoyed every one of our trainings, discussions, and meaningless and meaningful interactions.

I would also like to extend my gratitude to our dedicated technicians, Chi-Yuan Chang, Sylvie Taillon and Anik Chevrier for their assistance with biocompatibility tests, Noémie Laquerre, Maxime Beaudoin, Daniel Pilon, Matthieu Gauthier, and Philippe Plamondon. Their expertise greatly contributed to the advancement of my research.

I acknowledge the significant assistance of Carré Technologie and Biomomentum for their advice and crucial role in the course of my degree.

I am profoundly grateful to Professor Carlo Menon who provided me with an enriching opportunity to work in his group, the Biomedical and Mobile Health Technology Lab (BMHT), as part of an internship at the Swiss Federal Institute of Technology in Zürich. This internship offered me invaluable insights and growth opportunities

My sincere appreciation to Dr. Alexander Shokurov for his invaluable guidance, patience, and expertise which shaped my research skills and knowledge during my stay in Zurich.

I am also grateful to the BMHT team members for their warm welcome, collaborations and enriching discussions. Thank you, Veronika, Dr. Chakaveh, Dr. Moe, Alice, Dr. Sunil, Dr. Yinghong, Brett, Valeria, Maria, Xin, Carola, Lisa, Vera, Tomasz, Carmen, Valentina, Patricia, Lara, and Wenshan. I would also like to extend my gratitude to Dr. Karsten Kunze for his help and expertise.

I am grateful to Professor Marc Lavertu for allowing me to use his laboratories for biological experiments. I am also grateful to Professor Raphaël Trouillon and Professor Guillaume Majeau-Bettez for providing me the opportunity to work with their students. The chance to give back to other students in the framework of their courses has been deeply rewarding and insightful.

My appreciation extends to Professors Vahé and Chahé Nerguizian who have provided me with invaluable counsel and guidance throughout my academic journey.

I am deeply honored and very grateful to the Pierre Arbour Foundation, the Natural Sciences and Engineering Research Council of Canada (NSERC), and the Fonds de recherche du Québec – Nature et technologies (FRQNT) for supporting my Master's research, and MITACS for supporting my internship abroad. These financial supports have enabled me to focus on my research.

Lastly, I owe my deepest gratitude to my family and friends, without whom I would not be the person I am today.

I am indebted to all of you.

RÉSUMÉ

La surveillance des signes vitaux des enfants prématurés est d'une importance capitale pour leur santé. Les mesures de signaux électrophysiologiques nécessitent la mise en place d'électrodes sur la peau via un adhésif, ce qui peut entraîner des dommages car la peau des prématurés ne possède pas de couche externe protectrice. Par conséquent, des méthodes de surveillance alternatives sont nécessaires pour améliorer le confort et réduire le fardeau des prématurés. Cela peut être atteint avec des électrodes flexibles et étirables qui peuvent s'adapter à la forme et aux mouvements de l'enfant tout en maintenant la qualité du signal. À ce jour, quelques études ont été réalisées sur des électrodes à base d'hydrogel présentant d'excellentes propriétés mécaniques et électriques. Cependant, leur teneur en eau les rend sujettes à la dégradation par évaporation et donc inadéquates pour la surveillance à long terme.

Ce mémoire s'est concentré sur le développement et la caractérisation d'un matériau sec, imprimable, étirable, légèrement adhésif et auto-guérissant qui convient aux électrodes biomédicales pour les nourrissons prématurés. Cette recherche s'est appuyée sur les caractéristiques favorables du poly(3,4-éthylènedioxithiopène) dopé au sulfonate de polystyrène (PEDOT:PSS), un matériau conducteur dont les propriétés électriques et mécaniques peuvent être modifiées en fonction des additifs qui y sont ajoutés.

Dans ce travail, nous avons étudié l'incorporation du polyuréthane diol (PUD), du polyéthylène glycol (PEG) et du sorbitol au PEDOT:PSS afin de développer un mélange imprimable optimisé. Comme ces combinaisons améliorent considérablement les propriétés mécaniques et électriques du PEDOT:PSS, nous avons évalué ces propriétés à l'aide d'un testeur électromécanique. Nous avons également quantifié leur adhérence sur différentes surfaces afin d'évaluer leur compatibilité comme électrodes épidermiques.

En outre, nous avons évalué la biocompatibilité du matériau afin de vérifier son innocuité pour une application cutanée. Nous avons également démontré les propriétés d'autoguérison électrique du PUD/PEDOT:PSS.

L'application biomédicale potentielle de ce matériau a été démontrée par la fabrication d'une électrode épidermique imprimée sur un substrat de silicone étirable. Les électrodes résultantes présentent une impédance entre la peau et l’électrode comparable à celle d'une alternative

commercialisée et capturent avec succès des signaux physiologiques, y compris des signaux d'électrocardiogramme (ECG) et d'électromyogramme (EMG).

Le PUD, l'additif final ajouté au PEDOT :PSS et utilisé pour la fabrication de l'encre d'impression, a joué un rôle clé dans l’obtention des propriétés mécaniques et électriques, d'adhérence et d'autoguérison du matériau.

ABSTRACT

Monitoring vital signs of prematurely born children is of utmost importance for their health. The measurements of electrophysiological signals require the placement of electrodes on the skin via an adhesive, which can cause damage as premature skin lacks a protective outer layer. Therefore, alternative monitoring methods are needed to increase comfort and reduce the burden on premature infants. This can be achieved with flexible and stretchable electrodes that can adapt to the shape and movements of the child while maintaining signal quality. To date, a few studies on hydrogel-based electrodes with excellent mechanical and electrical properties have been reported. However, their water content makes them prone to degradation from evaporation, and therefore unsuitable for long term monitoring.

This study focused on the development and characterization of a dry, printable, stretchable, lightly adhesive, and self-healing material suitable for biomedical electrodes for premature infants. This research leveraged the favorable characteristics of poly(3,4-ethylenedioxithiopene) doped with polystyrene sulfonate (PEDOT:PSS), a conductive material with tunable electrical and mechanical properties depending on the used additives.

In this work, we explored the incorporation of polyurethane diol (PUD), polyethylene glycol (PEG), and sorbitol as additives to PEDOT:PSS to develop an optimized printable mixture. As these combinations significantly enhance both the mechanical and electrical properties of PEDOT:PSS, we evaluated these properties on an electromechanical tester. We also quantified their adhesion on different substrates to evaluate their suitability for epidermal electrodes.

Moreover, to verify the material's safety for skin application, we assessed its biocompatibility. In addition, we demonstrated the full electrical self-healing properties of PUD/PEDOT:PSS.

The potential biomedical application of this material was further demonstrated through the fabrication of a printed epidermal electrode on a stretchable silicone substrate. The resulting electrodes displayed skin-electrode impedance comparable to that of a commercially available alternative and successfully captured physiological signals, including electrocardiogram (ECG) and electromyogram (EMG) signals.

PUD, the final additive combined with PEDOT:PSS and used for the fabrication of the printing ink, played a key role in the mechanical and electrical, adhesion and self-healing properties of the material.

TABLE OF CONTENTS

LIST OF TABLES

LIST OF FIGURES

LISTE OF SYMBOLS AND ABBREVIATIONS

AE	Active electrode
Ag/AgCl	Silver/Silver chloride
ASTM	American Society for Testing and Materials
CE	Counter electrode
CNT	Carbon nanotube
CP	Conductive polymer
DIW	Deionized water
DMEM	Dulbecco’s phosphate-buffered saline
DMSO	Dimethyl sulfoxide
ECG	Electrocardiography
EDA	Electrodermal activity
EDOT	3,4-ethylenedioxythiopene
EDTA	Ethylenediaminetetraacetic acid
EEG	Electroencephalography
EMG	Electromyography
FBS	Fetal bovine serum
FTIR	Fourier transform infrared
GSR	Galvanic skin response
IPA	Isopropyl alcohol
ISO	International Organization for Standardization
K	Potassium
MARSI	Medical Adhesive-Related Injury
Na	Sodium

OECT	Organic electrochemical transistor
PAAM	Polyacrylamide
PANI	Polyaniline
PCB	Printed circuit board
PDMS	Poly(dimethylsiloxane)
PEDOT	Poly(3,4-ethylenedioxythiophene)
PEG	Polyethylene glycol
PMMA	Polymethylmetacrylate
PPy	Polypyrrole
PSS	Polystyrene sulfonate
PUD	Polyurethane diol
SEM	Scanning electron microscopy
TPU	Thermoplastic polyurethane
VPP	Vapor phase polymerization
WE	Working electrode

LIST OF APPENDICES

CHAPTER 1 INTRODUCTION

1.1 Electrophysiology

Electrophysiology is the study of the electrical and electrochemical events of biological tissues and the flow of ions going through them. This study encompasses the study of electrical currents in organs such as the heart, the brain or even the skin.

Electrophysiological signals are extracted from various techniques such as electrocardiography (ECG)[1, 2], electroencephalography (EEG)[3], electromyography (EMG)[4], and electrodermal activity (EDA)[5]. These signals serve as crucial measures in monitoring, diagnosing, or treating diseases[6] associated to the heart, brain, muscles, and skin respectively.

For the heart and muscles, ECG and EMG respectively are essential tools to translate their electrical signals. These electrical signals originate from the electrical activity of excitable cells such as the cardiomyocytes [7] for the heart. Ion channels in the cellular membrane of these excitable cells allow ions to flow through it.

At rest, there is an equilibrium of ions on both sides of the membrane with a slight charge difference, maintaining a rest potential. When a cell is activated, triggered for instance by a nerve signal, a rapid influx of positively charged ions, typically K^+ (potassium ion) flow into the cell, which creates a change in membrane potential and in turn generates an electrical signal [8, 9]. When many cells are activated, the combination of their ion flow, through volume conduction [10, 11], can be detected by electrodes placed on the skin.

In the case of the heart, the autonomous nervous system triggers the Purkinje cell, which are excitable cells that coordinate the contraction of the cardiac chambers. This response generates the distinctive PQRST peaks (Figure 1.1 PQRST complex of ECG) corresponding to the sequential contraction of the atria and ventricles.

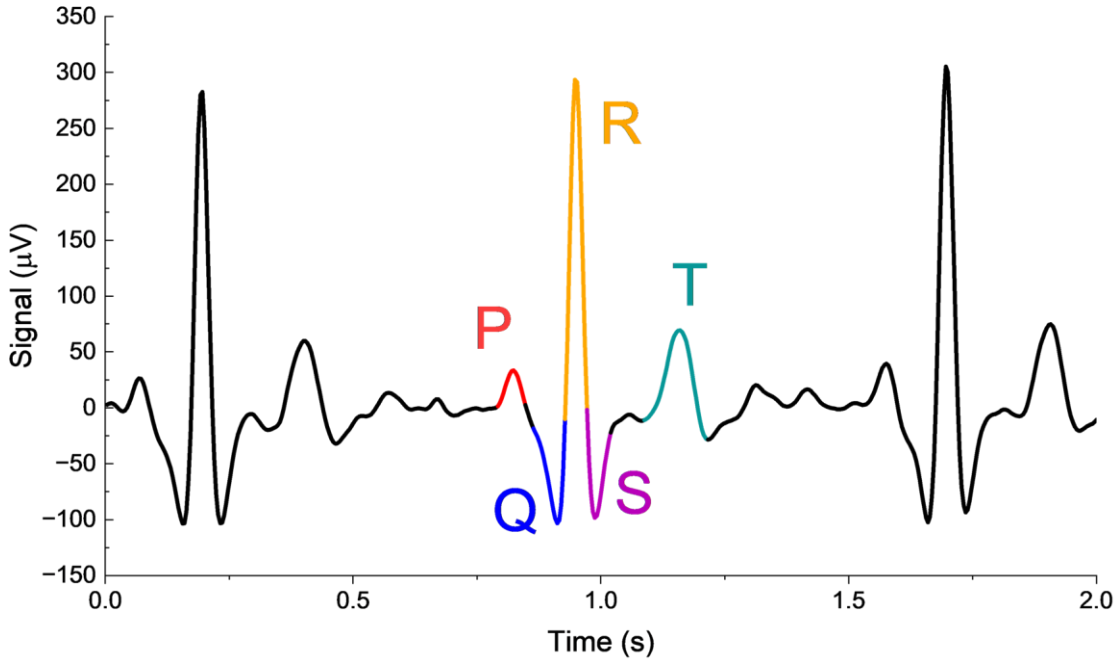

Figure 1.1 PQRST complex of ECG. Figure realized by the author.

The monitoring of these signals are vital for the diagnosis of cardiac or musculoskeletal conditions.

In the case of the brain, EEG is used to record the electrical activity of the brain. More precisely, when a neural cell is activated, there is a flow of ions across the neural membrane. This flow produces an almost infinitesimal electrical field, but when thousands or millions of neurons are activated, the sum of these electrical currents produces an electrical field strong enough to spread to the scalp surface which can be picked up by EEG electrodes [12, 13]. This signal provides valuable information about various neurological issues.

In the case of the skin, electrodermal activity (EDA) or galvanic skin response (GSR) is a general term for the electrical activity pertaining to sweat glands, and dermal and epidermal tissues. This activity is measured through the effect of moisture levels on the skin's conductivity. An increase in perspiration translates into an increase in the conductivity of the skin as the amount of electrolyte increases at the surface of the skin and allows for ionic conductivity. EDA or GSR are usually measured using two electrodes on the skin. By passing a small current through the skin

and measuring the resulting conductivity, an insight into the person's emotional state can be inferred. As sweat glands are controlled by the sympathetic nervous system, when a person experiences psychological stimulation such as stress or excitement, their sympathetic system triggers the activation of sweat glands, which increases the skin conductivity [5, 14, 15]. The most well-known usage for this signal is in polygraph tests.

The measurement of these signals in a non-invasive manner involves the use of epidermal electrodes.

1.2 Epidermal electrodes

Epidermal electrodes can broadly be classified into two main categories: wet and dry [16].

Wet electrodes, which refer to electrodes requiring the use of an electrolyte, are mostly made of hydrogels, which have found increased popularity in bioelectronics [17-19], specifically electrophysiology. Wet electrodes have garnered widespread commercial use as hydrogels offer adhesion and a good interface between soft tissue and metal electrode. In fact, commonly used silver/silver chloride (Ag/AgCl) medical electrodes consist of a metallic conductor (Ag) and an electrolytic hydrogel containing chloride ions. However, wet electrodes, and more generally gel-based electrodes, are commonly single-use and suffer from water-loss [20, 21].

Consequently, dry electrodes are a promising solution to the noted durability issue. Not only are they already extensively used and researched, but they also exist in various forms. Nonetheless, it is important to have a dry electrode that can closely adhere to the skin to improve the skin-electrode interface. Employing adhesive dry electrodes could effectively address this issue.

1.2.1 Conductive polymers in epidermal electrodes

Discovered through serendipity in the 70s [22, 23], conductive polymers (CP) revolutionized the field of electronics and started the field of organic electronics. CPs, notably poly(3,4-ethylenedioxythiopene):polystyrene sulfonate (PEDOT:PSS), have a great potential in the development of electrodes. Due to their biocompatibility, tunable mechanical and electrical properties, potential for self-healing ability, and their combined electronic and ionic conductivity, CPs provide an efficient interface between the skin and electronic devices. With these attributes, CPs emerge as a promising component for wearable bioelectronics, such as epidermal electrodes.

1.3 Skin of premature infants

Wearable electronics in sports, healthcare, and even daily life are becoming increasingly popular, and baby health monitoring as well as care for the elderly are a few of the many opportunities for wearables [24]. It is of paramount importance to design epidermal electrodes adapted to premature skin. As their skin is remarkably thin and susceptible to injury, they are at risk of skin damage, especially from adhesive-related injuries such as Medical Adhesive-Related Skin Injuries (MARSI) [25, 26], adhesives that often accompany epidermal electrodes. This is due to the lack of fully developed skin in preterm infants, mostly the top layer of the epidermis, the stratum corneum, which is the outermost layer of the skin that serves as a protective barrier. When conventional electrodes using regular adhesives are used for premature infants, it can lead to irritation or even skin breakdown.

Therefore, developing specialized epidermal electrodes is crucial to ensure the accurate physiological monitoring of premature infants while promoting their overall well-being.

1.4 Problematics

Vital signs monitoring in preterm infants is of crucial for their health. Electrocardiography (ECG), electroencephalography (EEG), heart rate, and respiratory data provide key insights into their well-being and developmental progress [27, 28]. These measurements require the application of electrodes to the skin using an adhesive, which can cause skin damage given the absence of a protective outer layer in premature infants' skin [27, 28]. This presents an obvious need for alternative monitoring strategies to increase comfort and reduce the burden of premature infants. This can be achieved with stretchable electrodes with tunable adhesion that can safely adhere and adapt to the contours and movements of the child while maintaining signal quality.

1.5 Objectives

The main objective of this thesis was to develop flexible and stretchable electrodes for premature infants. The following specific objectives were set to achieve the main objective:

1. Design flexible and stretchable material for non-invasive electrodes using conductive polymers

   We investigated the use of different additives such as sorbitol, polyethylene glycol (PEG), and polyurethane diol (PUD) added to a suspension of poly(3,4-ethylenedioxythiopene): polystyrene sulfonate (PEDOT:PSS).

2. Characterize the mechanical and electrical properties of the obtained material

   Employing a universal tensile machine, we analyzed the mechanical and adhesion properties of the produced materials. Additionally, we evaluated their electrical conductivity and electromechanical properties.

3. Validate the viability of the conductive polymer-based electrodes on human subjects

   The biocompatibility of the material was initially tested, followed by the use of the printing of the material to obtain epidermal electrodes. The practical application of the developed materials was validated by employing them as electrophysiological sensors.

1.6 Organization

This thesis starts with a literature review in Chapter 2 on the topics of conductive polymers, epidermal electrodes, and the skin. The literature review is followed by Chapter 3 which delves into printing and biocompatibility protocols. Notably, this chapter serves as supplement to Chapter 4 by detailing techniques that are not comprehensively explored within this chapter. Chapter 4 consists of an article reprinted for this thesis with detailed methods and materials used in the work as well as the main results and discussions. The article discusses the development of an epidermal electrode with properties relevant to the main objective of this thesis. Chapter 5 summarizes the conclusions and perspectives.

CHAPTER 2 STATE OF THE ART

2.1 Conductive polymers

Conductive polymers represent a family of organic materials able to conduct electricity. They were first discovered in 1977 with the synthesis of conductive polyacetylene [23]. This remarkable discovery of electrically conductive polymers led Professors Alan J. Heeger, Alan G. MacDiarmid, and Hideki Shirakawa to be recognized with the Nobel Prize in Chemistry in 2000. This discovery would give rise to the field of organic electronics.

Nowadays, the family of conductive polymers has expanded beyond polyacetylene to include poly(3,4-ethylenedioxythiophene) (PEDOT), polythiophene, polypyrrole (PPy), polyaniline (PANI), polyphenylene derivatives, among others.

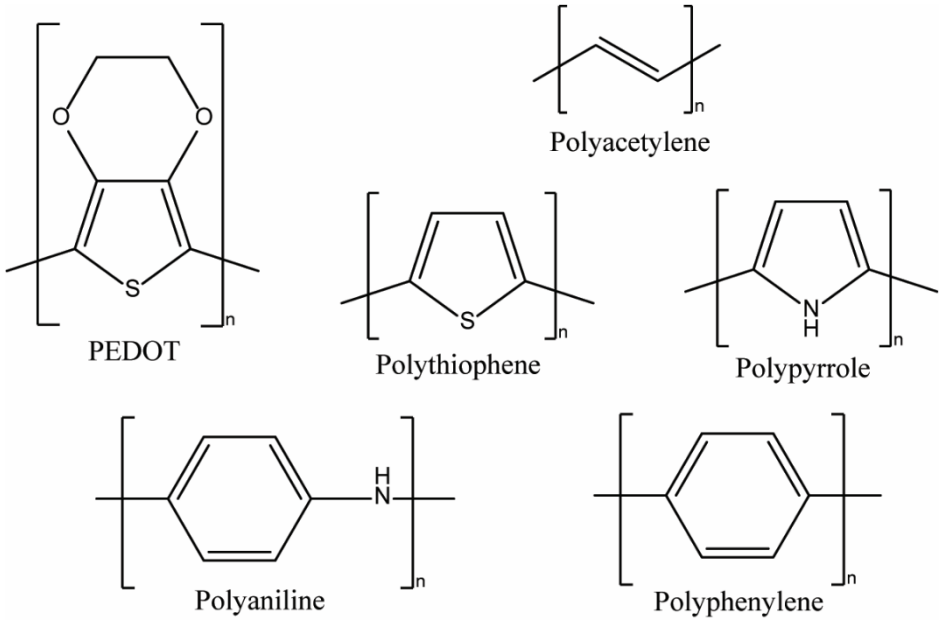

Figure 2.1 Structure of conductive polymers. Figure realized by the author.

Today, these polymers are researched for various applications, ranging from energy storage to flexible wearables. Their ability to be processed into flexible and stretchable devices, coupled

with their inherent electrical properties, makes them excellent candidates for innovations in the field of electronics, and more particularly bioelectronics.

This potential for bioelectronics stems from the biocompatibility of some conductive polymers, and their ease of processing, which allows for their successful integration into various bioelectronic devices [29-31].

2.1.1 Conductivity mechanism in conductive polymers

The fundamental property of CPs from which their conductivity arises is the presence of conjugated double bonds, π-bonds, along the backbone of these polymers. This structure comprises an alternating sequence of single and double bonds, with single bonds containing a σ-bond, and double bonds containing a σ-bond and a π-bond. Nonetheless, CPs remain very low in conductivity in their neutral or undoped state. Higher conductivities are achieved through chemical doping, not to confuse with doping in metals or semiconductors.

In CPs, single bonds, or σ-bonds, are strongly localized and are responsible for holding the polymer together, as opposed to π-bonds, which allow for the shared electrons to move freely between atoms [32, 33] To increase the conductivity of CPs and optimize the mobility of electrons, ions are incorporated in the polymer chain by removing electrons (oxidation), or adding electrons (reduction). In the case of a removed electron, a charge carrier such as a positive hole is created. This hole can move along the conjugated backbone of the polymer, leading to improved electrical conductivity.

Briefly, as illustrated for polyacetylene in Figure 2.2, when an electron is removed from an undoped conductive polymer, the added charge is known as a polaron. When a second electron is removed, we obtain a bipolaron, and by combining the radicals of both polarons, we obtain solitons, which will move during the application of an electrical potential and allow for electrical conductivity [32, 33].

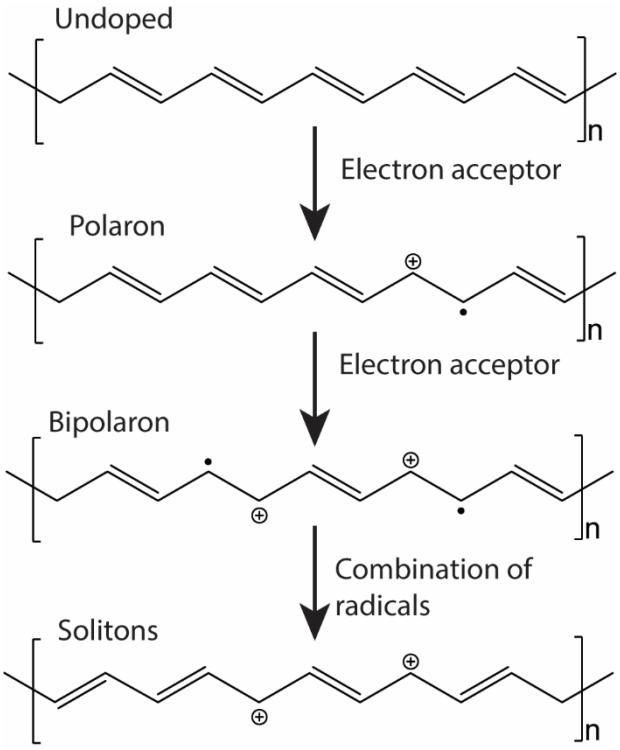

Figure 2.2 Doping of polyacetylene. Figure realized by the author.

The doping process involves a dopant which lead to the oxidation or reduction of the initial neutral polymer chain. As illustrated in Figure 2.3 with PEDOT:PSS, counterions, PSS^- in this case, balance the charge resulting from the doping process and maintain electrical neutrality [34].

2.1.2 PEDOT:PSS

PEDOT was first patented in 1988 by Bayer AG through the oxidative polymerization of 3,4-ethylenedioxythiopene (EDOT) [35] and has drawn a lot of attention due to its high conductivity and stability in ambient conditions [36]. A breakthrough was achieved by introducing PSS to PEDOT. PEDOT:PSS is a complex of the conductive polymer $PEDOT^+$ and the large dopant polymer PSS^- (Figure 2.3). In fact, $PEDOT^+$ is incorporated into the PSS^- polyanion matrix (Figure 2.4), as opposed to when PEDOT is doped with small anions. In fact, commercially available PEDOT:PSS dispersion have PEDOT chains with a molecular weight ranging from 1000-2500 g/mol and much larger PSS chains with a molecular weight of approximately 400 000 g/mol [37].

Not only this large polymeric dopant maintains electrical neutrality, but it also influences the overall processability properties of PEDOT [38, 39].

Indeed, PEDOT:PSS is mainly commercially available in water dispersion. As PEDOT alone is not water dispersible, this water stabilisation stems from the hydrophilic polymeric dopant, PSS, which has allowed PEDOT to become more easily solution processable with various printing, casting and coating methods [38].

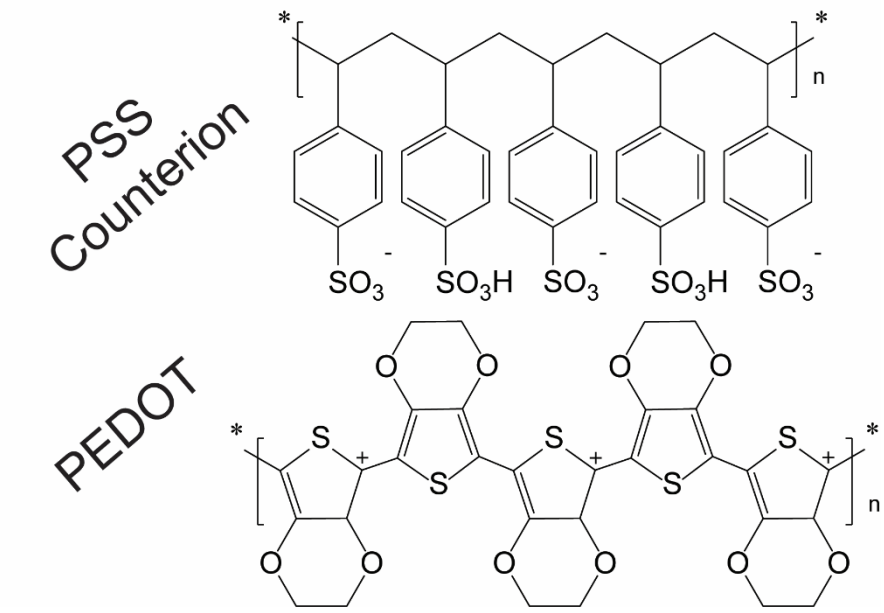

Figure 2.3 Conductive polymer PEDOT and counterion PSS. Figure realized by the author.

A notable additional advantage of PEDOT:PSS and most CPs is their capacity for combined ionic and electronic conductivity[29, 40, 41]. Chemical doping enables conductive polymers have ionic charges and to convert ionic currents into electric currents, therefore serving as excellent interface between biological tissues, which use ionic currents, and metallic electrodes, which use electronic currents.

Moreover, hydrating PEDOT:PSS creates ion-transport pathways which lead to ion mobility [42]. In the context of dry PEDOT:PSS-based films used as epidermal electrodes, sweat could act as hydration and external source of ions.

Furthermore, PEDOT:PSS is recognized for its self-healing properties, mainly due to the PSS chains. PEDOT:PSS demonstrated self-healing abilities upon the addition of water, attributed to the highly hydrophilic nature of PSS and its swelling capacity [38, 43].

2.1.3 Use of plasticizers or secondary dopants

A plasticizer is a substance incorporated into another material, typically a polymer, to increase its flexibility and overall softness [44]. This plasticization is achieved through the reduction of interactions between polymer chains which allows enhanced mechanical properties.

As pristine PEDOT:PSS lacks significant stretchability, plasticizers play a critical role in the fine-tuning of its mechanical properties by decreasing the Young's modulus and increasing the elongation at break [45-47]. Interestingly, plasticizer can also affect the conductivity of PEDOT:PSS.

A notable example of plasticizer is sorbitol, which, when added to PEDOT:PSS, which has a conductivity between 0.1 and 1 S/cm, allows for a stretchability over 60%, and a conductivity over 1000 S/cm [48]. Similarly, polyethylene glycol (PEG) at different molecular weight lower the Young's modulus and improve the conductivity [49].

He et al have also tested the use of glycerol, malic acid, 1,2,6-hexanetriol, and triethylene glycol, sorbitol, dimethyl sulfoxide (DMSO), triglyme, tetraglyme, formamide and 1-hexanol when added in amounts of 2% to PEDOT:PSS and they found that the enhancement of mechanical stretchability was more significant for compounds with multiple hydroxyl groups [50]. An elongation at break of more than 50% was measured for glycerol, triethylene glycol and malic acid, whereas other solvents had a lower elongation, around 30%, but still higher than pristine PEDOT:PSS (<10%).

In the case of fluorosurfactants such as Zonyl and Capstone, improvements in stretchability have been observed. For instance, Zonyl-enhanced PEDOT:PSS improved stretchability to about 50% but with no significant effect on conductivity [51], while Capstone-treated PEDOT:PSS resulted

in a stretchability of 38% and conductivity of 150 S/cm [52]. Another surfactant, Triton X-100, gave more than 50% elongation and a conductivity of around 80 S/cm [53].

The introduction of ionic additives has also been proven efficient, with Bao's group reporting ionic conductivities reaching 4100 S/cm and an elongation at break of 800% [54]. Their ionic nature allows these additives to simultaneously dope PEDOT and separate PEDOT and PSS.

As previously presented, PEDOT is integrated into a PSS matrix which allows for its dispersion in water. However, these ionic complexes form coils with hydrophilic PSS-rich shells shielding the hydrophobic PEDOT-rich core from the water. This insulating PSS becomes an obstacle to conductivity and explains the low conductivity of PEDOT:PSS (<1 S/cm). The addition of a plasticizer will screen the ionic interaction between PEDOT and PSS by forming hydrogen bonds with PSS, prompting the uncoiling of the shells and linearization of PEDOT chains and consequently an enhancement of conductivity [29, 39, 54, 55] (Figure 2.4).

Similar effects can also be achieved through solvent treatments with hydrophilic solvents like methanol, ethanol or isopropyl alcohol (IPA), or acid treatments, which will interact with PSS or remove it [39, 56].

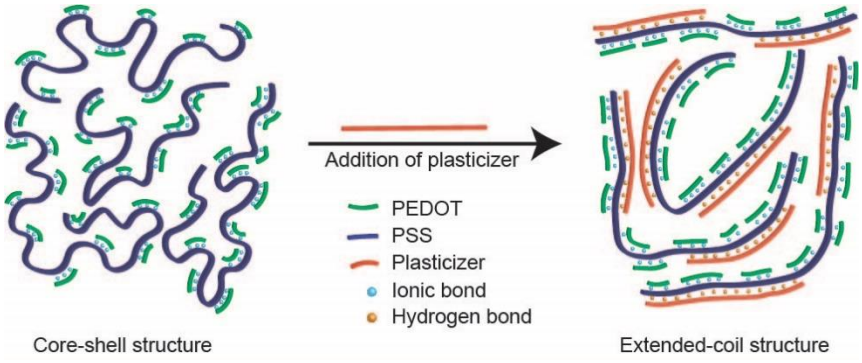

Figure 2.4 Effect of a plasticizer on the conformation of PEDOT:PSS. Figure realized by the author.

Furthermore, in the ongoing efforts to enhance the softness and stretchability of PEDOT:PSS, this CP has also been integrated into elastomeric materials such as polyurethane (PU) [57, 58] and polydimethylsiloxane (PDMS) [59, 60].

For example, Syeydin et al incorporated PEDOT:PSS with polyurethane and demonstrated an impressive elongation at break of more than 300% coupled with a conductivity of about 10 S/cm [57]. Zhang et al used a waterborne polyurethane (WPU) in combination with the plasticizer sorbitol to obtain a stretchability of 43% and a conductivity of about 350 S/cm [58].

The incorporation of PEDOT:PSS into silicones such as PDMS has also shown encouraging results. Luo et al reported a PEDOT:PSS/PDMS composite with low sheet resistance (20 Ω sq^{-1}) and an elongation at break around 82% [60].

To summarize, plasticizers incorporated into PEDOT:PSS significantly improve mechanical and electrical properties by disrupting interactions between $PEDOT^{+}$ and PSS^{-} chains.

2.1.4 Processing of conductive polymers

A main advantage of CPs is their flexible processing and the various methods available to deposit them on various substrates. These strategies include *in situ* deposition methods such as vapor phase polymerization (VPP) or electropolymerization, and *ex situ* polymerized CPs like dip-coating, casting and printing, which involves the polymerization of the CP before its application on the substrate. This section focuses on printing with PEDOT:PSS.

2.1.4.1 Printing

Printing provides a flexible, rapid, and low-cost approach to designing sensors meeting specific requirements of shape, size, and thickness. Our group has previously printed electrodes to monitor electrodermal activity [61] and printed organic electrochemical transistors (OECTs) [62, 63]. According to IDTechEx, a market research agency, printed, flexible and organic electronics is estimated to reach $73.3 billion by 2029 [64]. By printing electronics, complex processes such as lithography can be avoided. In fact, a significant advantage of printing includes the reduction in manufacturing steps, its ease of customization, and the ability to printing on different substrate such as textiles [65], PDMS, poly(eythylene terephthalate) (PET) and thermoplastic polyurethane (TPU) [61] and with a wide range of inks, including metallic and polymer-based inks [66]. Currently, printing is already used for the fabrication of wearables for vital sign monitoring [67]. Printing provides a significant opportunity for customizable circuits [68] and therefore personalized wearables.

There are various printing techniques available (Figure 2.5) with each their own advantages. Inkjet printing offers high-resolution and rapid patterning, which is ideal for work requiring precision such as microelectrodes [69]. Screen printing on the other hand provides the ability to deposit on large surfaces and opens the door to mass production [70]. Gravure printing also allows for upscaling with the added possibility of being integrated into roll-to-roll processing [71]. Blade-coating or doctor blade allows uniform thin coatings, and spray coating provides an easy technique to uniformly coat tridimensional substrates.

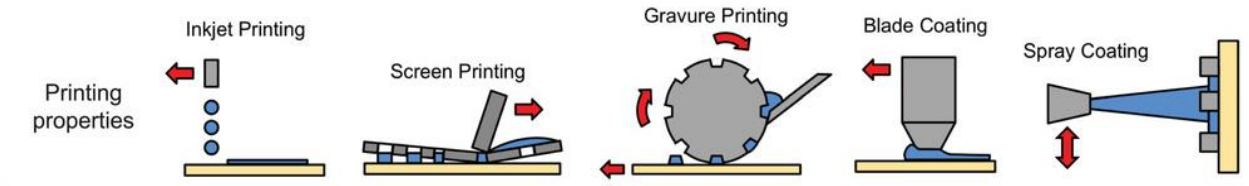

Figure 2.5 Different printing techniques. Inkjet printing, screen printing, gravure printing, blade coating, and spray coating. Reprinted with permission from [66]. Copyright © 2019, Wiley-VCH.

Direct write printing techniques such as inkjet printing allow direct patterning which eliminates the need for masks required for techniques such as lithography and screen-printing.

Self-healing printable electronics

Self-healing ability has emerged as a promising property of electronic devices, offering enhanced durability. This ability can be achieved through the use of conductive polymers such as PEDOT:PSS. The self-healing property of PEDOT:PSS holds great potential for various applications, including flexible electronics, wearable devices, and bioelectronics, where the ability to withstand mechanical deformation and maintain long-term performance is crucial. It offers opportunities for extending device lifetimes, improving reliability, and reducing the need for manual repairs or replacements, thus paving the way for advanced and resilient electronic systems.

The self-healing ability of conductive polymers refers to their capacity to repair damage and restore their electrical and/or mechanical properties, autonomously or with the use of external stimuli such as humidity, heat, or the addition of a solvent [43].

This ability arises from the reversibility of non-covalent bonds present a molecule's structure such as dynamic covalent bonds like Diels-Alder reactions, disulfide bonds or imine bonds as well as non-covalent bonds like hydrophobic interactions, hydrogens bonds, π-π stacking interactions, metal-ligand interactions, and ionic bonds [43]. In PEDOT:PSS, the self-healing behavior can be attributed to the dynamic interactions between the polymer chains through π-π stacking interactions, hydrogen bonding, and electrostatic interactions. These reversible bonds allow the conductive polymer to recover its electrical conductivity after sustaining damage.

Furthermore, when used in combination with additives such as plasticizers, the modification of mechanical properties such as the reduction in Young's modulus and increased viscoelasticity contribute to the self-healing capacity of the final material [43].

Regarding printed self-healing electronics, we have identified two primary approaches: self-healing electronics printed on a self-healing substrate and intrinsically self-healing material.

For the first approach, self-healable electronics relying on printing on self-healing substrates, Liu et al. achieved printable and self-healing electrical circuits by printing silver nanowires onto an elastic polyurea substrate which used polydimethylsiloxane (PDMS) as a soft segment and dynamic exchangeable urea or imine bonds and hydrogen bonds as self healing mechanism (Figure 2.6). As the printed silver layer and the substrate formed a strong interfacial adhesion when heated to 60°C, the substrate provided stretchability and self-healing ability to the printed layer [72].

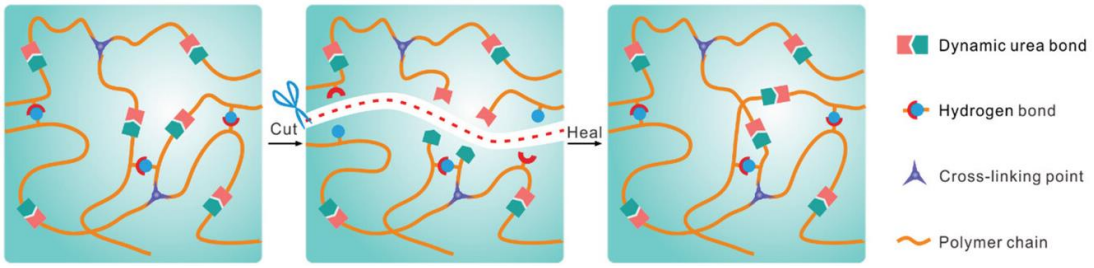

Figure 2.6 Schematic illustration of the dynamic urea bond and hydrogen bond during self-healing. Reprinted with permission from [72]. Copyright © 2021, Wiley-VCH.

Conversely, for the second approach which uses an intrinsically self-healing material, Seong et al. reported a self-healable ink using silver mixed with a gelatin scaffold (Figure 2.7a) which allowed the formation of new bonds upon heating [73]. Similarly, Ye and al reported an injectable conductive self-healing hydrogel for wearable electronics with applications in healthcare. To achieve this, an interpenetration polymer network consisting of multiwalled carbon nanotube, PEDOT:PSS, polyacrylamide (PAAM), poly(vinyl alcohol) (PVA) and borax was used to elaborate a hydrogel that can be printed [74]. Comparably, Su et al. implemented a blend of PEDOT:PSS and a soft polymer, (poly(2-acrylamido-2-methyl-1-propanesulfonic acid),

to create a self-healing stretchable channel material for OECTs [75] (Figure 2.7b). This blend was printed onto a styrene-ethylene-butylene-styrene elastomer using spray coating, demonstrating a viable printed and self-healing fabrication approach for electronics.

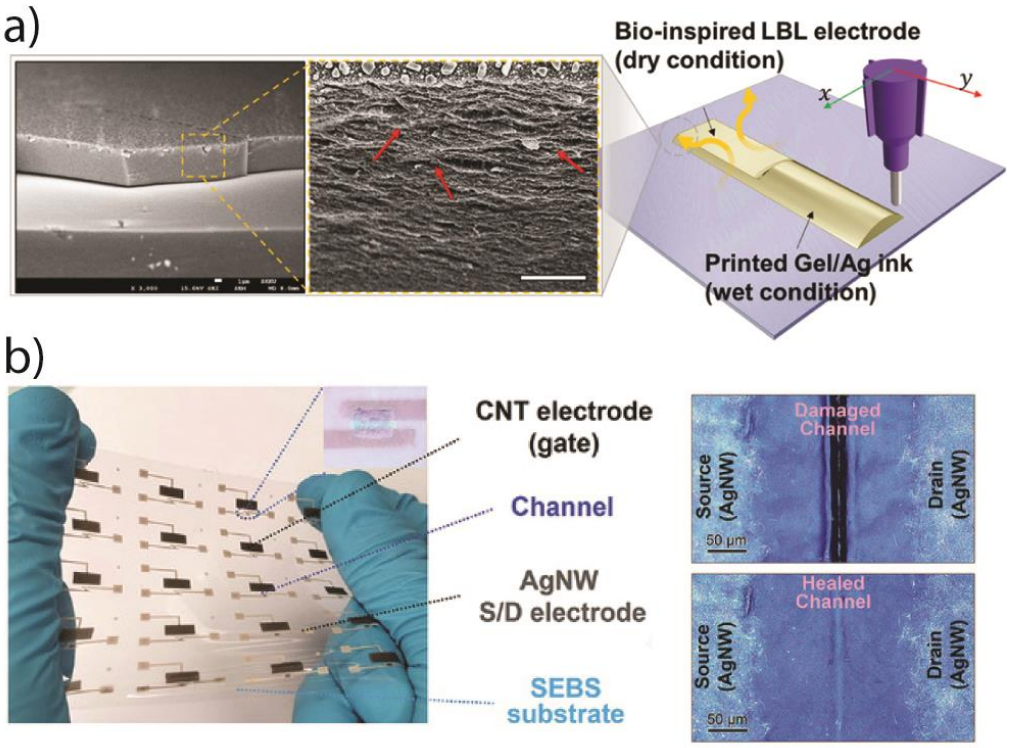

Figure 2.7 a) Schematic illustration of printing self-healing gelatin-silver ink and cross-sectional SEM images of the dried ink's structure with interpenetrating gelatin with silver particles. Reprinted with permission from [73]. Copyright © 2018, American Chemical Society. b) OECTS with self-healing PEDOT:PSS-based ink as channel material and optical image of the transistor before and after cutting, showing self-healing behavior. Reprinted with permission from [75]. Copyright © 2022, Wiley-VCH.

The advancements of self-healing printed electronics represent an important shift in the field of electronics. These innovations promise durable and reliable electronics resulting in reduced electronic waste combined with the rapid production arising from printability.

2.2 Epidermal electrodes

Monitoring the electrical activity of different organs such as the heart, muscles, brain, etc., is a key factor for early diagnostics. As discussed in chapter 1, non-invasive biopotential measurements occur through the detection of ionic current flow in the body using epidermal electrodes. In epidermal electrodes, this detection occurs at the skin-electrode interface and is quantified by the skin-electrode impedance which will be discussed in subchapter 2.2.3.

These electrodes can be divided into two categories: wet electrodes and dry electrodes. Wet electrodes are characterized by the presence of an ionic electrolyte, whereas dry electrodes are designed to operate without the need for external electrolytes. In the case of dry electrodes, sweat at the skin-electrode interface acts as the electrolyte [21]. The current trend in research is progressively going towards the use of dry electrodes, as the water dependency of wet electrodes makes them less durable and more susceptible to degradation due to water evaporation.

2.2.1 Dry electrodes

The simplest form of dry electrode is one that is solely comprised of a metal, as illustrated by the dry/stiff electrode in Figure 2.8. Bergey et al tested various metals as dry electrodes and found that stainless steel proved to be the most stable [76]. However, due to their stiffness and poor skin-electrode contact, they do not qualify as optimal electrodes. A great advantage of wet electrodes lies in their deformability, which allows them to conformably fit the irregular shape of the stratum corneum, the skin’s topmost layer. Further details on skin structure and characteristics will be presented in a subsequent chapter. As depicted in Figure 2.8, in contrast to dry and stiff electrodes, such as metallic ones, wet gel electrodes adapt to the skin and eliminate air pockets. These air pockets in dry and stiff electrodes reduce the effective contact area between the electrode and the skin, therefore lowering the signal quality. A potential solution to dry and stiff electrodes that do not require wet electrodes is the use of thin adhesive electrodes with high conformability to the uneven surface of the skin show potential for high quality measurements (Figure 2.8).

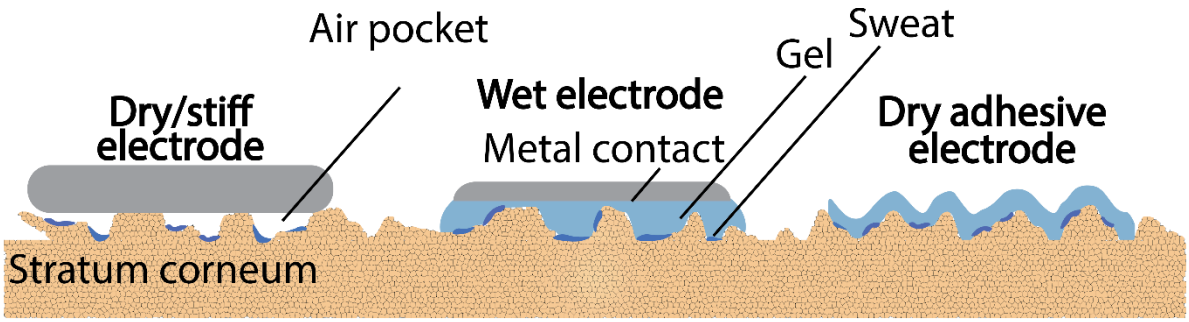

Figure 2.8 General types of epidermal electrodes. Figure realized by the author.

As is the case with EEG electrodes, there is a great variety of wet and dry electrodes (Figure 2.9) [16]. In the case of dry EEG electrodes, as there is a challenge in making contact with the skin because of the presence of hair, comb and bristle electrodes are used to penetrate the hair barrier and directly contact the epidermis. Microneedle electrodes go even further and pierce the skin barrier, the semi-permeable stratum corneum, to better measure ionic currents. Tattoo and dry adhesive electrodes allow for conformal contact with the skin but require to be placed on less hairy regions of the scalp.

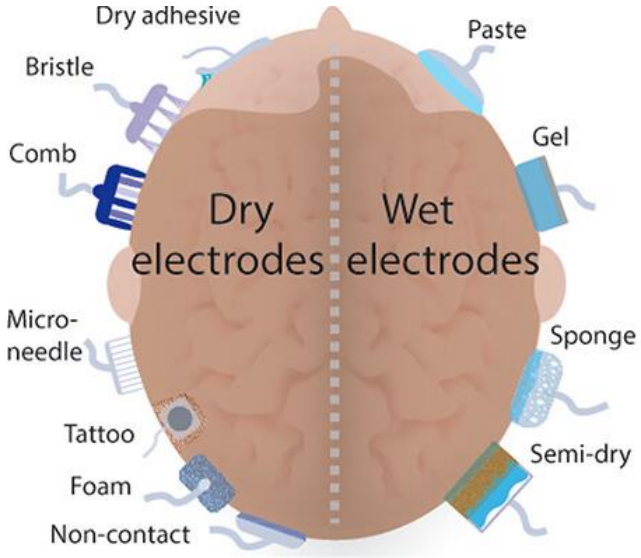

Figure 2.9 Different scalp EEG electrodes. Reprinted with permission from [16]. Copyright © 2023, American Chemical Society. Figure realized by the author.

A few dry electrodes are reported in **Table 1**. Among the types of dry electrodes, there are soft electrodes such as rubber-based ones. For example, Chen et al developed a composite rubber based on an ethylene propylene diene monomer (EPDM) matrix mixed with carbon to obtain a soft and conductive electrode [77]. Similarly, Jung et al blended PDMS, a silicone rubber, and carbon nanotubes (CNT) [78], whereas Wang et al sputtered gold on PDMS electrodes to obtain a flexible and dry electrode [79].

Conversely, textiles offer a great opportunity for wearables as the are comfortable and natural solution to long-term wear, making them an attractive choice for epidermal electrodes [80]. Numerous researchers have explored these dried epidermal electrodes; Haddad et al stitched Ag/AgCl e-textile onto woven textiles to measure EDA [81]. Bihar et al [65] successfully printed ECG electrodes using PEDOT:PSS on stretchable textile. In another instance, Takamatsu et al used a traditional Japanese textile processing technique to paint PEDOT:PSS onto fabric [82]. Pani et al used woven fabrics treated with PEDOT:PSS to record ECG [83]. Zhang et al polymerized PPy directly onto leather to obtain a durable and conformable ECG electrode [84]. These numerous advancements demonstrate the promising future of textile-based epidermal electrodes.

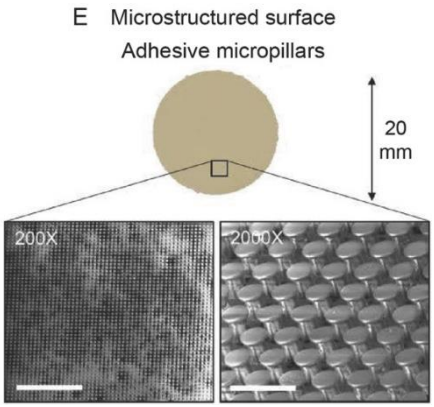

Figure 2.10 Soft dry electrode with adhesive microstructure surface. Reprinted with permission from[85]. Copyright © 2018, Wiley-VCH.

A potential obstacle with dry electrodes is the reduced contact with the skin. A solution would be to have adhesive dry electrodes. Posada-Quintero et al used a patented carbon salt and adhesive mixture for EDA measurements [86]. Stauffer et al fabricated a micro-pillar array using

photolithography and a PDMS and silver particles composite to obtain an adhesive electrode for ECG and EEG [85] which does not require the use of adhesives. Inspired by the feet of grasshoppers, the adhesion relies on the micro-pillar structure of the surface of the electrode which increase contact area with the skin.

Table 1. Current wet and dry epidermal electrodes

Type of electrode	Application	Materials	Reference	Year
Dry electrodes	ECG	Stainless steel electrodes	Bergey et al [76]	1971
	ECG and EEG	Ethylene propylene diene matrix with carbon	Chen et al [77]	2014
	EEG	CNT/PDMS composite	Jung et al [78]	2012
	EEG	PDMS coated with gold	Wang et al [79]	2012
	EDA	Ag/AgCl e-textile on woven cotton	Haddad et al [81]	2018
	ECG	Printed PEDOT:PSS on textile	Bihar et al [65]	2017
	ECG	Painted PEDOT:PSS on textile	Takamatsu et al [82]	2015
	ECG	PEDOT:PSS coated woven textile	Pani et al [83]	2015
	ECG	PPy polymerized *in situ* onto goat leather	Zhang et al [84]	2020
	EDA	Carbon salt and adhesive blend	Posada-Quintero et al [86]	2017
	ECG, EMG and EDA	PEDOT:PSS on textile	Sinha et al [87]	2020

	ECG and EEG	PDMS/silver particles-based micro-pillar structures fabricated using photolithography	Stauffer et al [85]	2018
Wet electrodes	ECG, EMG, and muscle stimulation	Gelatin/tannic acid with cholinium carboxylate ionic liquid	Aguzin et al [88]	2022
	ECG and EMG	PEDOT:PSS with PVA and borax	Zhou et al [19]	2022
	EMG	PEDOT:PSS gel and PVA/glutaraldehyde	Li et al [89]	2022
	ECG and EMG	Gelatin/PPy in glycerol/water	You et al [90]	2022
	EEG	Poly(n-acryloyl glycinamide)/potassium carbonate with glycerol	Shen et al [91]	2021

Additionally, having a material with similar mechanical properties to skin and able to conform to its stretchability is important. This can be achieved with PEDOT:PSS-based blends.

As a conductive polymer, PEDOT:PSS has gained substantial attention in recent research to fabricate electrodes for ECG, EMG, EEG and EDA applications (**Table 1**). Notably, PEDOT has shown a good adaptability for skin-electrode interface as well as conformability to soft tissues [92].

2.2.2 Wet electrodes

As previously discussed, wet electrodes rely on an electrolyte as ionic conductors to establish contact between the skin and the electrode. Most of wet electrodes are fabricated from hydrogels. In fact, Ag/AgCl electrodes, commonly used epidermal electrodes, consist of a metallic conductor paired with an electrolytic hydrogel containing chloride ions. Hydrogels are typically made of a polymer material that have the ability to absorb and retain large amounts of water. They are widely used in biomedical applications due to their similar mechanical properties to natural tissues, their conformability to skin, and their biocompatibility.

Several polymers including natural polymers such as gelatin, alginate, agar, and chitosan, and synthetic polymers such as polyacrylamide (PAAM) and polyethylene glycol (PEG). are used to fabricate hydrogel; Aguzin et al prepared gelatin based electrode with tannic acid as a cross-linker and cholinium carboxylate ionic liquids as electrolyte to record ECG and EMG as well as stimulate muscles [88]. Our group recently used PEDOT:PSS in a glycol dispersion with PVA and borax to obtain self-healing epidermal electrodes for ECG and EMG [19].

The combination of hydrogels offers a significant advantage through the combination of their mechanical properties. For example, deformable hydrogel networks that can dissipate mechanical energy such as alginate and chitosan combined with highly stretchable elastic hydrogels (Figure 2.11) such as PAAM can lead to tough hydrogels with improved elasticity [18]. One such hydrogel, or double network hydrogel, was used for electrophysiological measurements by Li et al by preparing PVA crosslinked with glutaraldehyde and PEDOT:PSS gel.

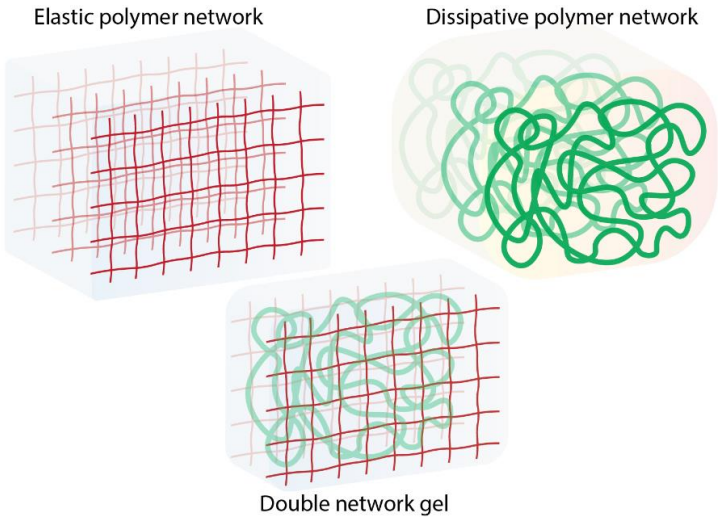

Figure 2.11 Illustration of double network gel through the combination of elastic and dissipative networks. Figure realized by the author.

One drawback of using hydrogels in epidermal electrodes is their susceptibility to drying out and deforming over time due to water loss. A solution is the use of organohydrogels which employ an organic solvent such as glycerol instead of water to form the gel. As most of these solvents have higher boiling points, they are less prone to drying out and losing their mechanical properties and ion mobility over time, which makes them a better alternative for long-term applications.

You et al developed a gelatin/PPy composite which was fermented with yeast and soaked in glycerol and water to obtain a porous organogel [90]. Shen et al also demonstrated the use of glycerol as an organic solvent in a polymerized n-acryloyl glycinamide network with potassium carbonate as a source of ions to obtain electrodes for long-term EEG [91].

To summarize, wet electrodes such as hydrogel-based ones offer interesting advantages due to their conformability to skin and similar mechanical properties to skin. Nonetheless, they present a major drawback in their short-term durability due to water evaporation. The use of less volatile solvents such as glycerol to form organohydrogels can overcome this limitation while offering similar electrical and mechanical properties as hydrogels.

2.2.3 Working mechanism of electrodes

To better understand the value of different types of electrodes, it is crucial to understand the skin and the underlying mechanisms involving the skin-electrode interface and the detection of ionic currents on the electrode, namely faradaic and non-faradaic processes. These mechanisms play a significant role in the signal quality. Moreover, PEDOT:PSS has shown a good adaptability for skin-electrode interface as well as conformability to soft tissues [92]. Its ability to lower skin-electrode interface impedance is an excellent advantage of PEDOT-based electrodes as it improves signal quality [83, 93]. This is due to the hybrid ionic and electronic conductivity of PEDOT:PSS, making it a perfect interface between the skin, which produces ionic currents, and the metallic electrodes, responsible for electronic current transport.

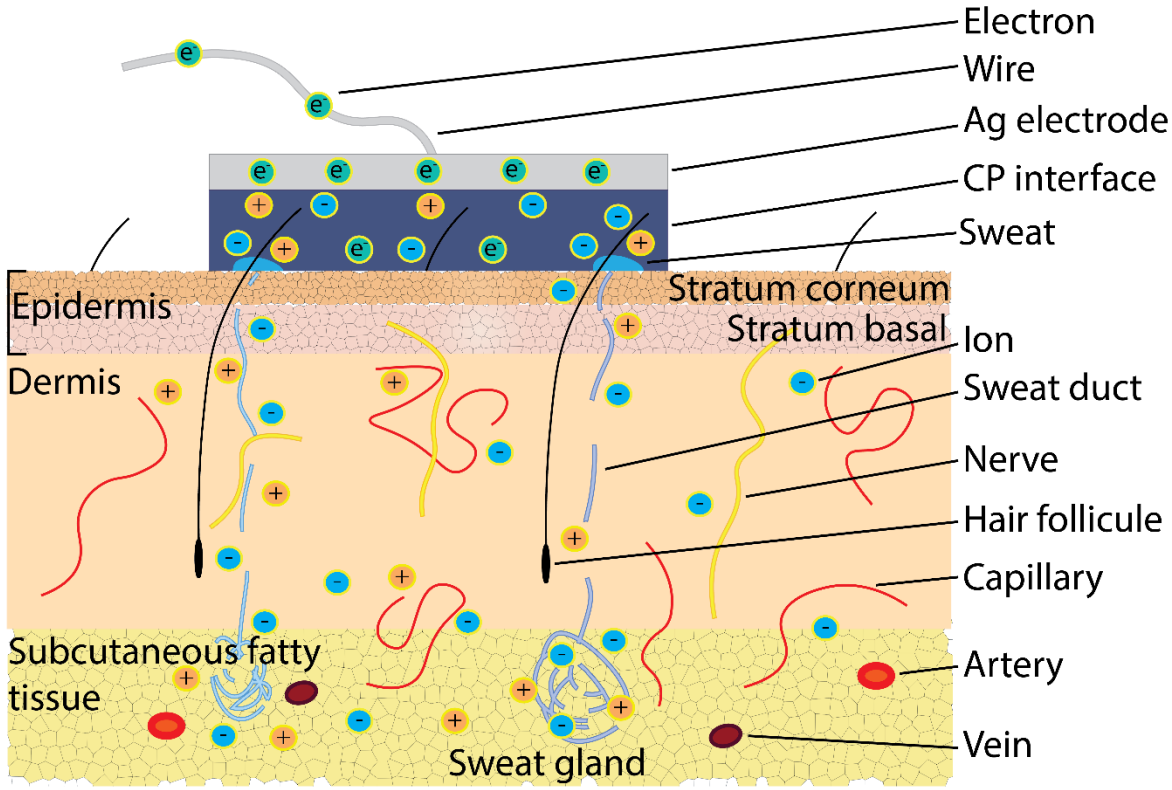

Figure 2.12 Illustration of skin structure featuring an electrode with conductive polymer interface and demonstrating ionic and electronic conductivity. Figure realized by the author.

The skin is constituted of three main layers (Figure 2.12), the epidermis which is the topmost layer and exposed to the environment. This layer protects against physical injuries and pathogens and is further divided into several sublayers, with the topmost layer being the stratum corneum. The second layer is the dermis, where important structures such as nerves, hair follicles, and sweat glands are located. The third layer is the subcutaneous layer, or hypodermis, which is mostly constituted of fat tissue.

Epidermal electrodes are necessary as an interface between the electronic device and the skin. However, the skin is only semipermeable to ions [21], as the outermost layer of the epidermis, the stratum corneum, is a layer of dead cells of 20 to 70 µm. Consequently, the primary pathway for ionic conductivity is via sweat glands [94]. Therefore, in the case of dry electrodes, perspiration will improve the skin's conductivity by penetrating into the pores of the stratum corneum, and therefore increasing and improving the effective contact area between the electrode and the skin [21]. Often, the skin is also abraded to remove some of the stratum corneum and improve signal quality.

The fundamental mechanisms for current transfer from the biological tissue to the electrode involve Faradaic and non-Faradaic processes [94-96]. When an electrode is in contact with an electrolyte, such as bodily fluids rich in charged ions like sodium ions (Na^+) and chloride ions (Cl^-), the charge transfer across this interface follows Faraday's Law. According to this law, the amount of chemical reactions resulting in charge transfer is proportional to the current flowing through this interface. Briefly, in this process, charges such as electrons or ions cross the skin-electrode interface through electrochemical reactions: oxidation and reduction. In the case of a current direction towards the electronic signal acquisition device, reduction accounts for the majority of chemical reactions [97]:

$$n + e^- \rightarrow n^-$$

$$n^+ + e^- \rightarrow n$$

Where "n" is a neutral atom or molecule, "e^-" is an electron, and "n^+" and "n^-" are charged atoms or molecules, as illustrated in Figure 2.13a. When obeying Faraday's Law, this skin-electrode

interface behaves as a resistance (Figure 2.13b). In the case of an oxidation reaction such as electrostimulation, the arrows' direction would be reversed.

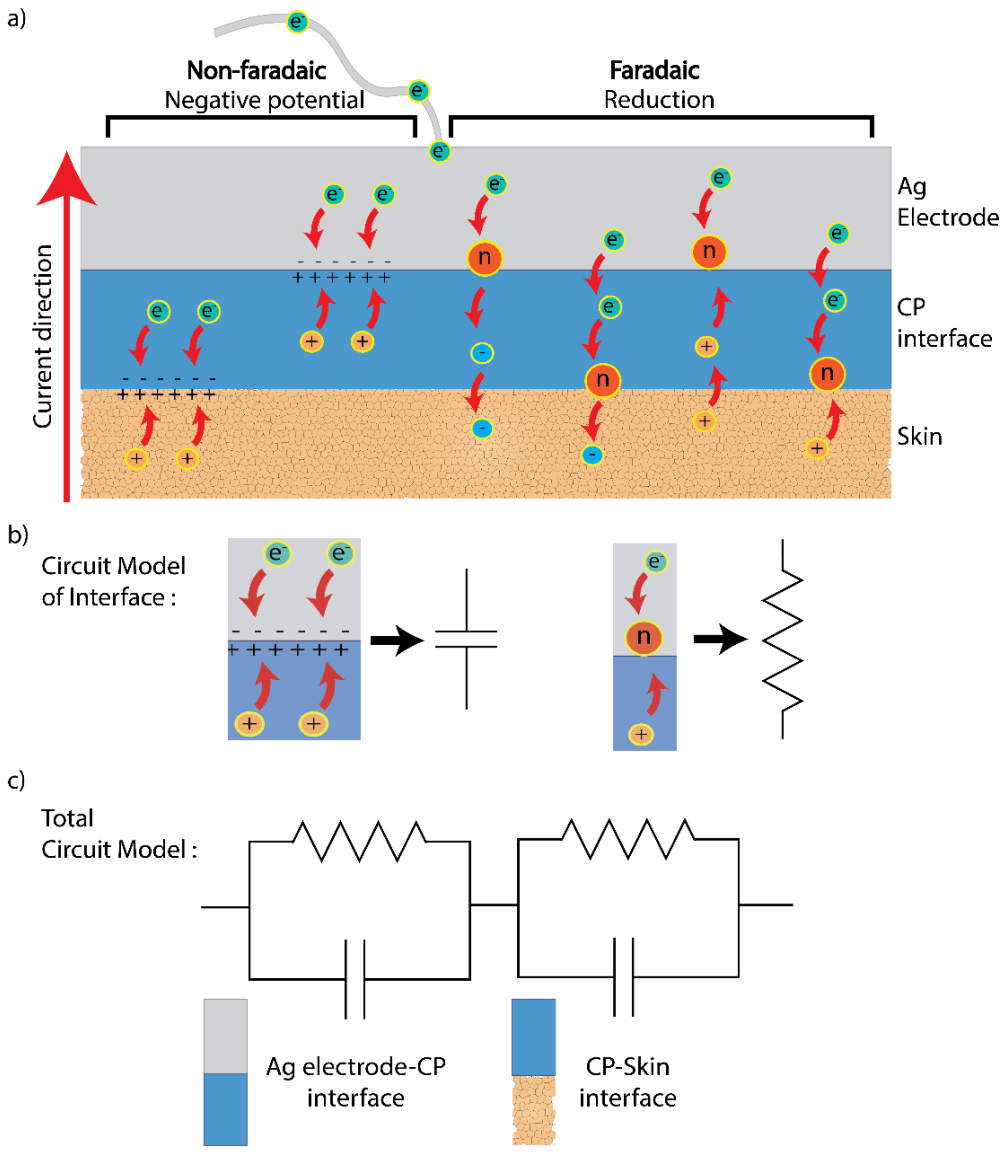

Figure 2.13 Working mechanism of epidermal electrodes with a) illustration of non-Faradaic and Faradaic processes, b) equivalent electrical circuit for non-Faradaic and Faradaic processes, and c) total electrical equivalent circuit of the skin-electrode interface. Figure realized by the author.

Another mechanism occurring in epidermal electrodes involves the non-Faradaic process, where charges never cross the interface, but accumulate at it, thus polarizing the electrode (Figure

2.13a). The non-Faradaic process behaves as a capacitance (Figure 2.13b). PEDOT:PSS, with its dual ionic and electronic conductivity, enables these mechanisms to occur at both interfaces: between the metallic part of the electrode and the CP interface, and the CP and the skin (Figure 2.13a). Hence, there are two sets of Faradaic and non-Faradaic interfaces. As both the resistance (a Faradaic process) and the capacitance (non-Faradaic process) occur in parallel at the metal/CP interface and subsequently at the CP/skin interface, the total equivalent circuit [98] can by depicted by a resistance and capacitance in parallel, and in series with another parallel pairing of resistance and capacitance (Figure 2.13c).

The quality of the skin-electrode interface represented by the equivalent circuit in Figure 2.13c, which is an important aspect of acquiring reliable physiological signals, is typically quantified through the measurement of the skin-electrode impedance. A lower impedance indicates a better interface and higher signal quality.

2.3 Premature skin and adhesion

Owing to their sensitive skin, [27, 99] preterm infants could benefit from the development of soft bioelectronics because of the tunable adhesivity, stretchability, and other mechanical properties of soft organic electronics and conductive polymers [31, 100] PEDOT:PSS.

To address the specific requirements of premature infants' skin, it is important to understand the substantial differences between the skin of a premature infant and adults, as well as when compared to newborns.

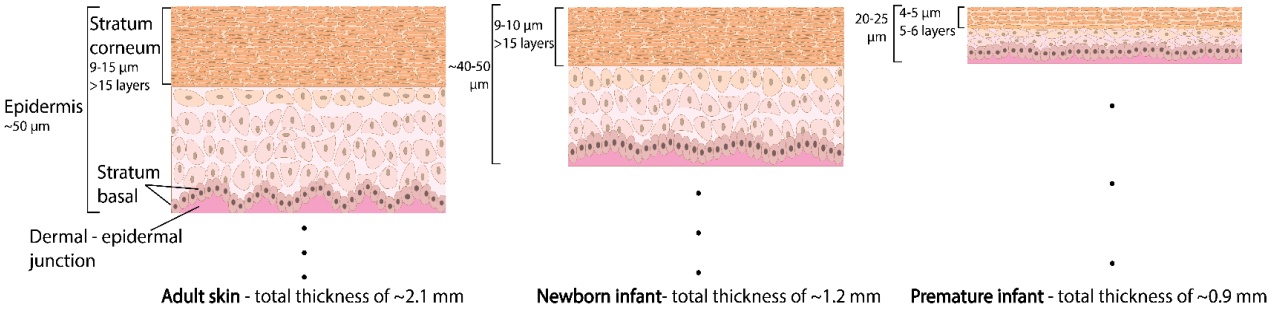

Figure 2.14 Top skin layers of adults, newborns and premature infants and their respective thicknesses. Figure realized by the author.

The thickness and properties of each layer of the skin varies across different stages of human development (Figure 2.14). In adults, the total thickness reaches 2.1 mm, whereas for newborns, this thickness is of 1.2 mm and only 0.9 mm for premature skin [101]. The most significant difference in premature skin is noticed for the epidermis, the topmost layer of the skin, where adults and newborns have similar thickness, about 50 µm, but premature have less than half, falling in the range between 20 and 25 µm. This disparity is even more noticeable when looking at the stratum corneum, which is approximately 3 times thinner in premature infants than in adults [101]. The stratum corneum is crucial in protecting the body from loss of water, pathogens and injuries [102].

Moreover, in the context of non-invasive electrophysiology, the stratum corneum presents the most significant obstacle to signal acquisition, as its roughness, semipermeability to ions and presence of sweat greatly impact the quality of the signal. Some procedures in adults even require

the abrasion of the stratum corneum before the application of electrodes. Conversely, in more invasive approaches such as microneedle electrodes used for EEG, this skin layer is bypassed by piercing it and enabling direct contact with the underlying layer which exhibits higher permeability to ions transporting electrophysiological signals.

Another aspect of the skin requiring careful consideration in preterm infants is the dermal-epidermal junction, which is the boundary between the outer epidermis and the underlying dermis (Figure 2.14). Initially, premature skin presents lesser and smaller desmosomes, which are structures responsible for intercellular adhesion [101, 103]. Thus, premature skin is very susceptible to peeling off as the bond between adhesive and stratum corneum might be stronger than between epidermis and dermis [104]. This may result in the removal of the epidermis and reduced protective function of the skin, or more generally medical-adhesive related skin injuries (MARSI) when using regular medical adhesives.

Furthermore, on one hand, due to the vulnerability and thinness of premature skin, special care needs to be given to the chemical composition of electrode materials, as certain substances can easily permeate the skin [105]. For instance, the use of borax should be avoided due to its potential to cause renal failure, whereas glycerol and propylene glycol, common ingredients in epidermal electrodes, ionic pastes and emollients, are to be avoided as they can results in hyperosmolarity (higher concentrations in blood) [105].

On the other hand, achieving quality measurements requires adequate adhesion to skin. However, electrodes that are paired with strong adhesives have been found to cause skin irritation [106] as well as MARSIs [25, 26, 107]. Consequently, the need for electrodes exhibiting moderate adhesion is evident.

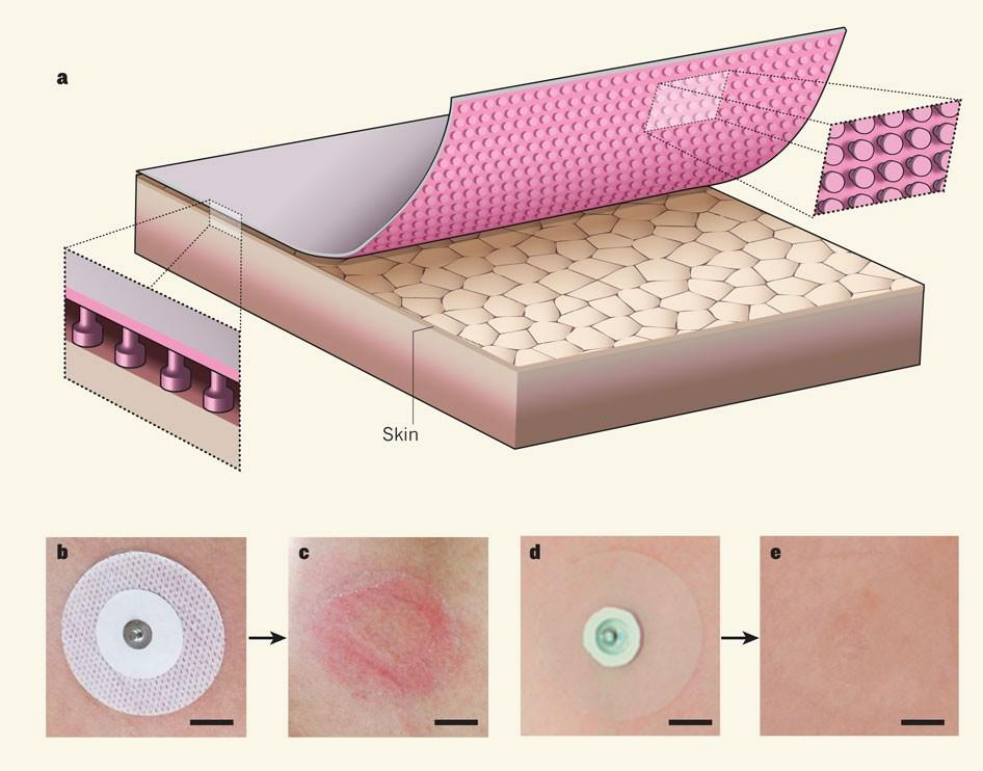

Figure 2.15 a) Glueless adhesive based on microstructured surface. B) acrylic adhesive leaving residue and causing redness (c), compared to (d,e) microstructured glueless adhesive with reduced redness. Reprinted with permission from [106] and [108]**.** Copyright © 2011, Springer Nature Limited and Wiley-VCH.

In recent years, there has also been research into the use of adhesive-less adhesives, such as micropillar-based structures [85, 108], which are inspired by the adhesive pads on the feet of insects. These types of adhesives use van der Waals forces to adhere to the skin and can be easily and painlessly peeled off (Figure 2.15). Adhesive-less adhesives have the potential to be more comfortable and less irritating for the patient.

Moreover, recent years have seen increased attention to research on different skin adhesives using acrylic, rubber, polyurethane and other strategies tailored for medical applications [109].

CHAPTER 3 MATERIALS AND METHODS

This section provides an overview of methods utilized in Chapter 4 but were not exhaustively detailed as they were not relevant to the main focus of the work. They are given more comprehensive attention here.

3.1 Direct-write extrusion printing

The Voltera V-One printed circuit board (PBC) printer is a direct-write printer that offers a resolution of 200 μm [110]. However, achieving this resolution requires the careful calibration of the printer's parameters before each printing session.

Three parameters influence the printing process of the Voltera: printing height, ink pressure, and printing speed. Prior to printing, the printer is calibrated by taking into account the specific substrate and ink, by fine-tuning the printing height and the extrusion pressure. The printing height is the distance between the extruder's nozzle and the substrate. High deposition leads to inadequate adhesion of the printed pattern, whereas low deposition causes the ink to be smeared across the substrate, potentially causing damage. This height might also depend on the adhesion of the substrate and the consistency of the ink. The printing height is generally set around 0.1mm but can greatly vary from silver inks to PEDOT:PSS-based inks.

Ink pressure constitutes another crucial parameter. More viscous inks require increased pressure for continuous and effective extrusion. However, too much pressure might result in broader tracks and consequently lower resolution, whereas low pressure will lead to discontinuous tracks.

Finally, printing speed, generally set at 500 mm per minute, can also impact print quality. Similar to ink pressure, slower printing speeds risk producing broader tracks, while higher speeds could lead to discontinuous tracks. However, when dealing with highly viscous and almost elastic inks, it is crucial to reduce the speed to allow time for the ink to adhere to the substrate. Higher speed would cause the ink to stick to the nozzle instead of the substrate, leading to the same discontinuous tracks.

In the case of hydrophobic substrates, surface treatment of the substrate can improve printability. For instance, one solution is to expose the surface to UV/O_3 thereby making it more hydrophilic and allowing easier adhesion of the ink on the hydrophobic surfaces. Alternatively, an

intermediary layer with good adhesion to the substrate could be printed on the hydrophobic surface before printing the final ink.

3.2 Biocompatibility

To validate the suitability of PEDOT:PSS-based films for use as epidermal electrodes, their biocompatibility on cells needs to be confirmed. Therefore, viability tests were carried out on C2C12 mouse myoblast cells. These myoblast cells were specifically seeded instead of epithelial cells as they have been previously used with other PEDOT:PSS suspensions [111, 112]. The protocols for thawing the purchased cells, subculturing them and conducting the viability tests on PEDOT:PSS-based mixtures are detailed here.

3.2.1 Thawing C2C12 cells

C2C12 cells in a 1mL aliquot were procured from ATCC in a frozen state and immediately stored in liquid nitrogen vapor phase (-180°C) upon reception. It is expected to have 1 million cells in 1mL of C2C12 solution. Subsequently, the vial containing the cells was thawed in a deionized water (DIW) bath at 37°C in less than 2 minutes with the exterior of the vial decontaminated with ethanol. The cells were transferred into a centrifuge tube containing 9 mL of Dulbecco's Modified Eagle's Medium (DMEM, ATCC) and centrifuged at 200 g for 5 minutes. By this point, the cells are expected to be aggregated at the bottom of the tube and the supernatant should contain the solvents that were used to preserve the cells at low temperatures. The supernatant was discarded, and the cells were carefully resuspended in 9 mL of DMEM with 10% of Fetal Bovine Serum (FBS, ATCC). Ideally, around 1 million cells, or 100 000 cells per mL are in this solution. Finally, 2mL of the obtained solution were added to 10 mL of warmed complete medium (10% FBS in DMEM) and plated in a T75 Nunc Delta flask (Nunc™, Thermo Fisher Scientific) and placed in an incubator under a constant temperature of 37°C in a humidity-saturated environment (95% air / 5% CO_2).

This culture was subcultured every two to three days once the culture reached a confluency of 50-70%, meaning that most cells are physically touching each other.

3.2.2 Subculturing

As it is important to keep the cells healthy for the viability test, it is important to passage them before they reach 60% confluency (full or 100% confluency would be when 100% of the plate is covered with cells) as they already start to differentiate and fuse together when they reach this level in their growth.

To passage the cells, their culture media was removed using vacuum with a Pasteur glass pipet. The surface of the T75 flask on which the cells are attached were rinsed twice with Dulbecco's phosphate buffer saline without calcium or magnesium (DPBS). This step removes the proteins on the cells that would inhibit the enzyme, trypsin, to break down the proteins enabling the adhesion of the cells onto the flask. Prewarmed 1 mL of 0.25% (w/v) of trypsin with 0.53mM EDTA solution (Gibco) was added onto the cells and rapidly observed under an inverted microscope. As the adhesion proteins are slowly broken, the cells are expected to change shape from flattened to round. The cells, still in the T75 flask are placed in the incubator for 2 minutes. It is important not to leave the cells exposed to trypsin for too long as the enzyme could slowly damage the membrane of the cells and cause their death. Once removed, the flask is gently hit in different directions to ensure the complete detachment of cells. This can be confirmed by the observation of floating round particles under the microscope.

Once the cells are detached, the trypsin is inactivated by adding 9 mL of complete medium (DMEM with 10% FBS). The cell solution is transferred into a sterile tube. A small fraction of the solution is used to count the concentration of cells using the hemacytometer test as we want to inoculate the next passage with 1.5×10^5 and 1.0×10^6 live cells per T75 flask ($75cm^2$).

A calculated quantity from the solution is diluted in another solution of complete medium for a total of 12 mL, added into a new sterile T75 flask and place into the incubator.

3.2.3 Viability test on PEDOT:PSS-coated samples

A sterilized mixture of PEDOT:PSS with different additives was coated onto microwell with 5 µL followed by drying at 70 °C overnight. Prior to cell plating, the PEDOT:PSS-coated microplates were rinsed thoroughly in DPBS media to remove any residues. Cells were seeded on PEDOT:PSS-coated wells as tests and on uncoated PS wells as controls. After cell growth, negative control wells were treated with IPA to kill the cells, while untreated and uncoated wells were used as positive controls. To study cell viability, a density of 10 000 cells per well was seeded on the microplates and cultivated for one day, 3 days, and 5 days. For each measurement, the culture media was removed from the microwell and rinsed with 100 µL of DPBS to remove extracellular factors that might react with the dye. Cell straining was conducted with a live/dead calcein AM/ethidium homodimer assay according to the manufacturer's instructions. After rinsing the samples, 100 µL dye (4 µM EthD-1 and 2 µM calcein in DPBS) was added in the microwell and incubated at 37°C for 30 min before observing under fluorescence. Cell observations were made using a fluorescence microscope (EVOS M5000, Thermo Scientific, USA). The images were acquired using GFP and Texas Red EVOS light cube filters for calcein and EthD-1 respectively. For quantitative cell viability, the cells were plated in black microplates for spectrophotometric measurement on a microplate reader (Infinite 200 Pro, Tecan, Switzerland). The fluorescence of the solutions was measured at 494 nm excitation and 517 nm emission. The cell viability, expressed as the percentage of live cells was then calculated as follows:

$$\%\ live\ cell = \frac{F(517)_{sam} - F(517)_{min}}{F(517)_{max} - F(517)_{min}}$$

Where $F(517)_{sam}$, $F(517)_{max}$, and $F(517)_{min}$ are the fluorescence of calcein AM on PEDOT:PSS-coated wells, positive control wells, and negative control wells, respectively.

CHAPTER 4 Article 1: Printable, adhesive, and self-healing dry epidermal electrodes based on PEDOT:PSS and polyurethane diol

Printable, adhesive, and self-healing dry epidermal electrodes based on PEDOT:PSS and polyurethane diol

Pierre Kateb[1], Jiaxin Fan[1], Jinsil Kim[1], Xin Zhou[1], Gregory A. Lodygensky[2] and Fabio Cicoira[1*]

[1]*Polytechnique Montréal, 2500 Chemin de Polytechnique, Montreal, Quebec H3T 1J4, Canada*

[2]*CHU Sainte-Justine Research Center, Department of Pediatrics, University of Montréal, 520 Rue Bélanger, Montreal, Quebec H1T 1C9, Canada*

**Email: fabio.cicoira@polymtl.ca*

Submitted July 28, 2023 Materials Today Communications

HighlightsHI

- Introducing polyurethane diol (PUD) as an additive to PEDOT:PSS can improve its mechanical, electrical, and self-healing properties
- Dry and adhesive electrodes were fabricated for electrophysiological measurements using PUD and PEDOT:PSS
- Printed and stretchable PEDOT:PSS/PUD epidermal electrodes were demonstrated

Keywords: PEDOT:PSS, electrophysiology, printable electronics, stretchable bioelectronics, polyurethane

Abstract

Printable, self-healing, stretchable, and conductive materials hold tremendous potential for the fabrication of advanced electronic devices. One such material, poly(3,4-ethylenedioxithiopene) doped with polystyrene sulfonate (PEDOT:PSS) has been the focus of extensive research due to its tunable electrical and mechanical properties. Due to its solution processability and self-healing ability, PEDOT:PSS is an excellent candidate for developing printable inks. In this study, we developed a printable, stretchable, dry, lightly adhesive, and self-healing material for biomedical use. Polyurethane diol (PUD), polyethylene glycol (PEG), and sorbitol were investigated as additives to PEDOT:PSS. Our research identified an optimal printable mixture obtained by

incorporating PUD with PEDOT:PSS, which improved both mechanical and electrical properties. Based on our optimization, for 5% PUD/PEDOT:PSS free-standing films, a conductivity of approximately 30 S/cm, a stretchability of 30% and a Young's modulus of 15 MPa were observed with a light adhesion of 0.03 N/cm. A low resistance change (< 20%) was achieved when stretched up to 30% of strain. Excellent electrical stability under cyclic mechanical strains, biocompatibility, and 100% electrical self-healing were also observed. The potential biomedical application of this mixture was demonstrated by a printed epidermal electrode on stretchable silicone substrate. The PUD/PEDOT:PSS electrodes displayed similar skin-electrode impedance to commercially available electrodes, and successfully captured physiological signals. This work contributes to the development of improved customization and enhanced mechanical durability for soft electronic materials.

4.1 Introduction

The conducting polymer, poly(3,4-ethylenedioxythiopene) doped with poly(styrenesulfonate) (PEDOT:PSS), is the subject to widespread research due to its versatility in electronic and biomedical applications [16, 59, 113]. The ability to achieve enhanced electrical conductivity, stretchability, and self-healing properties upon addition of other compounds makes PEDOT:PSS attractive for electrophysiological sensors and bioelectronics. Proper adhesion, mechanical properties resembling those of biological tissues, and the self-healing ability of the material are key factors in improving the reliability and prolonging the lifespan of such electronic devices. We previously reported reversibly stretchable conductive films obtained by printing a commercial PEDOT:PSS ink on thermoplastic polyurethane. This method was used to develop an electrodermal activity (EDA) sensor. However, ensuring optimal skin contact required a Velcro strap [61]. Another approach to promote contact with skin is fabricating adhesive and soft PEDOT:PSS-based hydrogels. By adding poly(vinyl alcohol) (PVA), β-cyclodextrin and citric acid, Tan *et al.* crafted a highly stretchable (700%), conductive (1-37 S/cm), low modulus (56.1-401.9 kPa), and adhesive (~4 N/cm) PEDOT:PSS-based composite, which was also used to make solution-processed adhesive conductive gel electrodes for soft electronics [114]. Recently our group [19] has successfully produced a self-healable, adhesive, conductive, and stretchable

PEDOT:PSS-based hydrogel by mixing PVA and borax with a commercial PEDOT:PSS suspension in glycols (diethylene glycol and propylene glycol). The use of hydrogel as a material for epidermal electrodes was also demonstrated. Considering the potential issues of water loss in ambient environments, the development of dry adhesive conductive materials with appropriate mechanical properties presents a more viable path for long-term soft device applications [21, 58, 85]. Building on this premise, Zhang *et al.* [17] combined waterborne polyurethane (PU) and D-sorbitol with PEDOT:PSS to create highly conductive, stretchable, and adhesive films. These films could be employed as dry electrodes for capturing electrocardiography (ECG) and electromyography (EMG) signals with low noise level and skin-electrode impedance.

PEDOT:PSS can be processed via various techniques. Specifically, interest is mounting in the development of printable materials with high conductivity, stretchability, and self-healing capabilities, given that printing offers a cost-effective and customizable path to mass production [68]. PEDOT:PSS is an excellent material for printable [61-63] and self-healing [19, 49, 115, 116] electronics. By blending PEDOT:PSS and a soft polymer, (poly(2-acrylamido-2-methyl-1-propanesulfonic acid), Su *et al.* printed a stretchable self-healable channel material for organic electrochemical transistors [75]. Ye *et al.* reported an injectable conductive self-healing hydrogel for wearable electronics with applications in healthcare, by using an interpenetrating polymer network consisting of multiwalled carbon nanotubes, PEDOT:PSS, polyacrylamide, PVA and borax [74]. Excellent mechanical and electrical properties, in addition to printability, self-healing, and adhesion, were achieved using a mixture of PU and PEDOT:PSS [46, 58, 117]. PU has been extensively used in biomedical applications and provides many advantages, such as biocompatibility, potential biodegradability, and tunable chemical and physical properties [118-120].

In this study, we employed polyurethane diol (PUD) to enhance both the stretchability (~30%) and electrical conductivity (~30 S/cm) of PEDOT:PSS, foster light adhesion (< 0.04 N/cm) on fake skin and instilling electrical self-healing capabilities. Furthermore, PUD with PEDOT:PSS allowed for a conductive polymer ink to be produced. PUD was selected due to its water solubility, with the aim to develop sustainable conducting polymer inks. The PUD/PEDOT:PSS films exhibited tolerance to repeated strains, electrical stability under mechanical cycling, and

biocompatibility. Additionally, we developed printed PUD/PEDOT:PSS epidermal electrodes on a flexible silicone substrate, with a skin-electrode impedance comparable with commercial Ag/AgCl gel electrodes and stable ECG and EMG signal recording. These findings highlight the potential of PUD/PEDOT:PSS to measure high-quality epidermal biopotential signals. This research endeavor paves the way for improved customizability, enhanced durability, and minimized discomfort in epidermal electrodes.

4.2 Experimental section

4.2.1 Chemicals and materials

Polyethylene glycol (PEG) 400 and polyurethane diol (PUD) were purchased from Sigma-Aldrich. PEDOT:PSS aqueous suspension (Clevios PH1000, PEDOT concentration of about 1-1.3 wt.%) was supplied by Heraeus Precious Metals. Sorbitol was purchased from Caledon Laboratories Ltd. The stretchable silver ink, used to print the metal contact for the electrodes was donated by Chimet S.p.A (Italy). A silicone elastomer kit (SYLGARD® 184), purchased from Dow Corning (USA), was used to prepare polydimethylsiloxane (PDMS). Polybutylene adipate terephthalate (Ecoflex™ Gel), used as the adhesive layer, was purchased from Smooth-On (USA). S mm flange (14SF-9 STUD-SS) and eyelets for studs (11 EYELET-R-NIC), were purchased from Rome Fastener Corporation (USA). A silicone-based “fake skin” with softness and stretchability similar to those of human skin was purchased from PIXESTT on Amazon. For the biocompatibility test, a C2C12 muscular mouse cell line was purchased from ATCC (USA). Dulbecco’s phosphate buffer saline (DPBS) powder without magnesium or calcium was purchased from Gibco. Nunc™ Nunclon Delta-treated flat-bottom 96-well plates from Thermo Fisher Scientific (USA) and OptiPlate™-96 Black from Perkin Elmer (USA) were used for cell culturing. The LIVE/DEAD Viability/Cytotoxicity Kit for Mammalian Cells (calcein AM/ethidium homodimer assay) was supplied by Thermo Fisher.

4.2.2 Preparation of thin films and epidermal electrodes

Free-standing Films

To understand the effect of each component on the adhesion, electrical, mechanical, and self-healing properties of the materials, 12 different mixtures of PEDOT:PSS, PUD, PEG, and

sorbitol were prepared. Their compositions are listed in **Table 2**. The chemical structures of the materials are shown in Figure 4.1a.

Table 2. Composition of the different PEDOT:PSS mixtures for electrical and mechanical characterizations.

	PUD (wt%)	PEG (wt%)	Sorbitol (wt%)	PH1000 (wt%)
2% PUD	2	0	0	98
5% PUD	5	0	0	95
10% PUD	10	0	0	90
2% PEG	0	2	0	98
2% PEG/2% PUD	2	2	0	96
2% PEG/5% PUD	5	2	0	93
5% PEG	0	5	0	95
2% sorbitol	0	0	2	98
2% sorbitol/2% PUD	2	0	2	96
2% sorbitol/5% PUD	5	0	2	93
5% sorbitol	0	0	5	95
Pristine PEDOT:PSS	0	0	0	100

Each mixture was stirred in a sealed vial at 1000 rpm using a magnetic stirrer for 30 min on a hot plate at 160 °C. Then, 2 g of the solution were poured into a 40 mm x 55 mm x 1 mm polymethylmethacrylate (PMMA) mold and heated at 70°C for 4 h in an oven to remove water

and obtain a dry film. This annealing temperature was used to avoid damaging the mold (PMMA softens above 80°C) and deteriorating the mechanical properties of the films, which are sensitive to high temperature treatment. The obtained films were cut using a razor blade into 10 mm by 40 mm strips, which were used for electrical and mechanical characterizations.

Epidermal Electrodes

The stretchable substrate was prepared by pouring PDMS base and curing agent (10:1) into a PMMA mold, degassed for 1 h to remove air bubbles and cured at 70°C in an oven for 4 h. Ecoflex was drop-cast over the PDMS, degassed, and cured at room temperature for 4 h. This procedure yielded 1 mm thick double-layered stretchable substrates, where the Ecoflex side was lightly adhesive, while the PDMS one was non-adhesive. The non-tacky PDMS layer facilitates demolding of the adhesive Ecoflex gel and acts as a carrier substrate for the entire structure, enhancing overall handling and maneuverability. The electrodes were printed on the adhesive side.

To prepare the PUD/PEDOT:PSS ink, the solution of PEDOT:PSS with 5% PUD, selected for electrode experiments, was heated to remove 50% by weight of the water, to obtain the higher viscosity required for printing. The resulting ink was filtered using a syringe filter (Chromspec UV syringe filters, 25 mm diameter and 5 µm pore size) to remove large particles.

Using a printed circuit board (PCB) printer (Voltera V-One, Canada), a layer of stretchable silver was first printed on the Ecoflex/PDMS substrate as the metal contact and cured at 50°C for 15 min. The silver layer was not fully cured in this step, as it would be heated after printing the PEDOT:PSS layer. The PUD/PEDOT:PSS ink was printed on top of the stretchable silver to form the active part of the electrode (diameter of 19 mm) and heated at 80°C for 120 min. Finally, snap buttons were installed using a Benchtop Model RFC03 (Rome Fastener Corporation, USA) to connect the electrodes to the ECG, EMG and skin-electrode impedance characterization devices.

4.2.3 Characterizations and measurements

Mechanical, Electrical, and Electromechanical Testing

For each mixture listed in **Table 2**, three different films with a width of 10 mm, a distance between grips of 10 mm, and different thicknesses listed in Table S1 were used for mechanical characterizations. A Mach-1 V500csst MA009 instrument, Biomomentum Inc. (Canada), was used for the tensile, electro-tensile and adhesion measurements. The thickness used to calculate the conductivity and Young's modulus was measured with the Mach-1 Biomomentum using an indenter with a 1 mm diameter tip. A 70 N and 1.5 N load cells were used in a uniaxial strain at a ramp rate of 1 mm/min. The load cell was calibrated prior to each use. The ramp rate and number of samples were set according to the ASTM 882 standard.[121] A four-point probe configuration was used to measure the variation of resistance during the tensile testing using a Keysight B2902A. This same system was used to measure the initial resistance of films at different voltages, from which the conductivity was calculated using the following equation based on Ohm's law:

$$\sigma = \frac{L}{R \cdot A} \qquad (1)$$

where σ is the conductivity, L is the length of the sample, R is the measured resistance, and A is the sample cross-sectional area. For testing the resistance change under cyclic stretching and strain-stress testing, the measured resistances were normalized as R/R_0, where R_0 is the initial resistance measured before mechanical tests.

The adhesion force was measured following the *Standard Test Method for 90 degree Peel Resistance of Adhesives*, ASTM D6862.[122] A free-standing PEDOT:PSS-based rectangular film of 65 mm x 10 mm was adhered onto glass or fake skin and then peeled at an angle of 90° between the substrate and the film and a rate of 50 mm/min for a length of 5 cm. The same test was repeated three times for each PEDOT:PSS-based mixture, and the error bars represent the standard deviation. The same test was performed for the Ecoflex/PDMS substrate, using the Ecoflex as the adhesive side, to get a reference value for the adhesion force.

Thermogravimetric Analysis (TGA)

Thermogravimetric analysis (TGA) was performed with a TG Q500 (TA Instruments, USA) to estimate the water content and understand the bonding between PUD and PEDOT:PSS. Three samples were used: 5% PUD, pristine PEDOT:PSS, and pristine PUD. 5% PUD/PEDOT:PSS

and pristine PEDOT:PSS films were prepared using the heating conditions described earlier, and the pristine PUD sample was heated at 100°C overnight to remove the solvent. 10 mg of each dried sample was analyzed in a platinum pan for a temperature range of 40 to 800°C (heating rate of 10°C min^{-1}) under nitrogen atmosphere (flow rate of 60 mL min^{-1}).

Fourier Transform Infrared sSpectrophotometry (FTIR)

The IR spectra of the films were collected with a Perkin Elmer FTIR Spectrum 65 for a range of 600 to 4000 cm^{-1} at a resolution of 4 cm^{-1} for 16 scans.

4.2.4 Electrical self-healing measurements

Self-healing measurements were performed on free-standing (5% PUD/PEDOT:PSS, 5% PEG/PEDOT:PSS and 5% sorbitol/PEDOT:PSS) and printed (5% PUD/PEDOT:PSS) films with dimensions of 10 mm x 40 mm. The free-standing films were placed onto a microscope glass slide while the printed films were directly printed on glass. Two tungsten probes (Imina Technologies, Switzerland) placed at the two ends of the film were used to establish the electrical contacts. A constant voltage of 0.2 V was applied to the film by a Keysight B2902A source/measurement unit, and the electrical current was continuously monitored during the process. For the 5% sorbitol/PEDOT:PSS film, which exhibited low conductivity (as reported in Table S 3), an applied voltage of 2 V was used for the self-healing tests. The cuts were created manually using a razor blade (Ultrasource Single Edge blade 500205), yielding a size of approximately 20 µm. Multiple cuts were created at various locations on the film. Each cut was made after the current stabilized. All the experiments were carried out under ambient conditions.

4.2.5 Biocompatibility

Cell culture was performed by seeding C2C12 cells (mouse muscle cells) on PEDOT:PSS-coated 96-wells. About 5 µL of 5% PUD/PEDOT:PSS solution was used to coat a 96-well, which was subsequently dried in sterile conditions and then washed with DPBS to remove residues. To quantify the viability of cells on the PUD/PEDOT:PSS, a live/dead calcein-AM/ethidium homodimer (EthD-1) assay was performed after 3 days and 5 days. Black 96-well microplates were used for fluorescence measurements with a Tecan Infinite 200 Pro microplate reader (Switzerland) at excitation/emission wavelengths of 494/517 nm and 528/617 nm for calcein and

EthD-1, respectively. For the fluorescence microscope, the images were acquired using GFP and Texas Red EVOS light cube filters were used for calcein and EthD-1, respectively, with an EVOS M5000 Invitrogen inverted benchtop microscope (USA).

4.2.6 Biopotential and skin-electrode impedance measurements

For biopotential and skin-electrode impedance measurements, we followed previously reported protocols [19]. Shortly, OpenBCI Cyton device was used to measure ECG and EMG at a sample rate of 250 Hz. For the ECG, the electrodes were placed on the left and right arms, and the reference electrode was placed on the right leg. A band-pass filter from 5 to 50 Hz, a notch filter at 60 Hz, as well as a gain of 24 were used. The signal baseline correction and the ECG complexes superposition were performed using an opensource Python toolbox for physiological signal, neurokit2 [123]. For the EMG, the active electrodes were placed on the biceps, 5 cm apart, and the reference on the elbow. A band-pass filter of 15 to 50 Hz was used and the signal was post-processed using the Python toolbox BioSPPy [124].

The skin-electrode impedance was measured with an electrochemical workstation (VSP-300, BioLogic, France) and a setup of three electrodes (working, reference, and counter electrodes) placed linearly on the forearm of a volunteer, at 6 and 12 cm from the first electrode. The PUD/PEDOT:PSS composite electrode (diameter of 19 mm) was used as the working electrode, while two commercial dry Ag/AgCl silicone gel electrodes (Natus, diameter of 19 mm) were used as reference and counter electrodes. The skin-electrode impedance was measured from 1 Hz to 100 kHz at 10 mV. All the skin-electrode impedance measurements were collected on the same volunteer at the same location and on the same day.

4.3 Results and discussion

4.3.1 Film and electrode fabrication

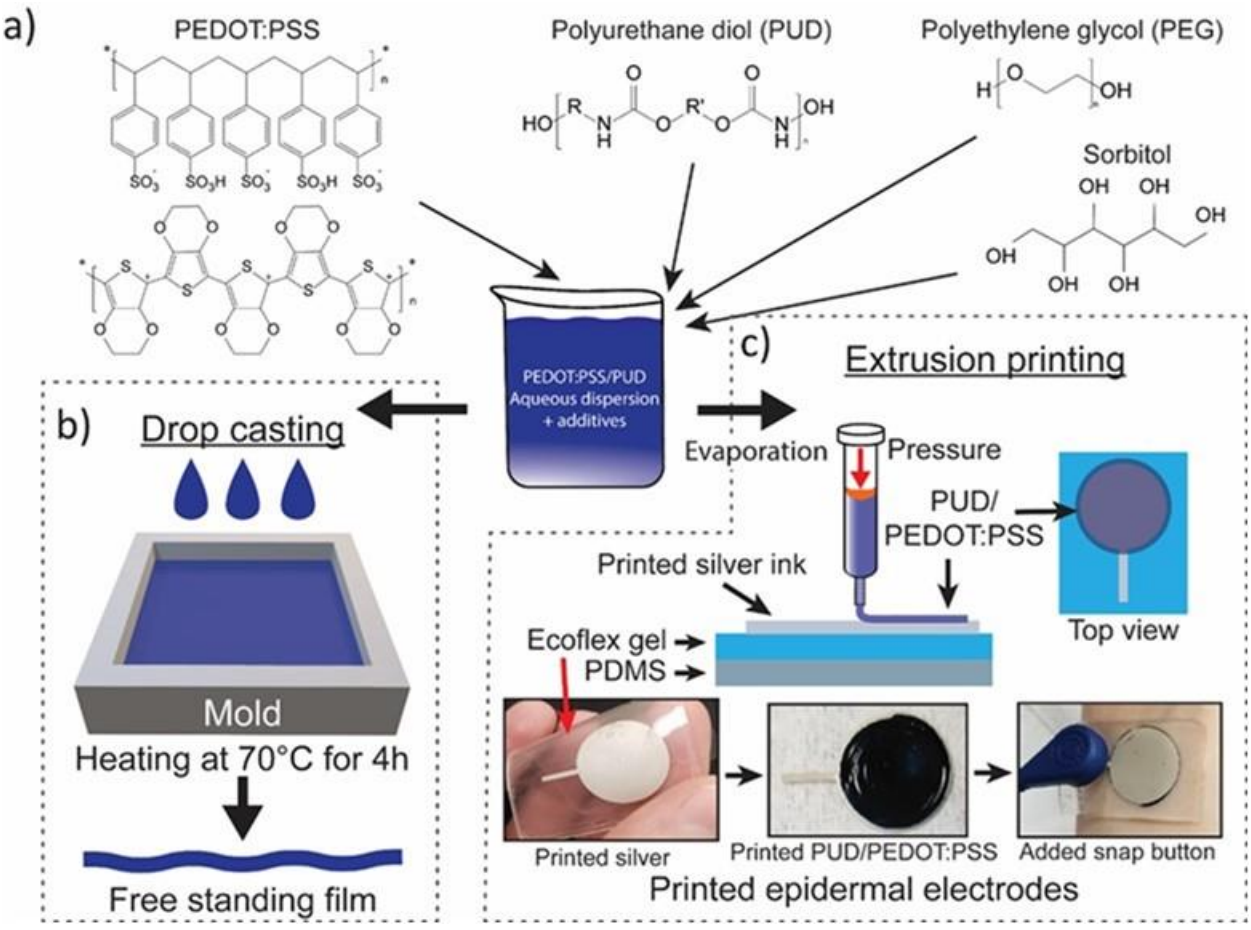

Figure 4.1 Schematic illustration of the fabrication process. A) Chemical structures of PEDOT:PSS, PUD, PEG, and sorbitol. B) Free-standing film preparation by drop casting the different PEDOT:PSS based mixtures listed in Table 1 in a PMMA mold. C) Printing of the PUD/PEDOT:PSS based epidermal electrode on PDMS/Ecoflex substrate. Photographs of printed silver, PUD/PEDOT:PSS printed on top of silver, and complete epidermal electrode with snap button added.

Epidermal electrophysiological electrodes require adhesion, suitable Young's modulus, stretchability, and low skin-electrode impedance for the attainment of reliable signal transmission. We opted for PEDOT:PSS as the electrode material due to its tunable electrical

conductivity and mechanical properties, which can be achieved upon the incorporation of other materials. PUD, PEG, and sorbitol were mixed with PEDOT:PSS to investigate their impact on the electrical and mechanical properties and achieve optimal adhesion, stretchability, electrical conductivity, self-healing performance, and biocompatibility. PEG has previously been demonstrated to enhance the conductivity of PEDOT:PSS films and their self-healing properties, with an effect on their Young modulus and elongation at break [49], whereas sorbitol is recognized to improve conductivity, adhesion and stretchability [48, 58]. We combined these three additives to PEDOT:PSS, in an attempt to improve both mechanical and electrical properties. Free-standing films (Figure 4.1b) were prepared for the assessment of material properties. We subsequently printed electrophysiological electrodes using the optimized formulation (Figure 4.1c). Our epidermal electrode consists of an elastic Ecoflex/PDMS substrate, electrical interconnects based on the stretchable silver ink, and a PUD/PEDOT:PSS top layer.

4.3.2 Mechanical characterization

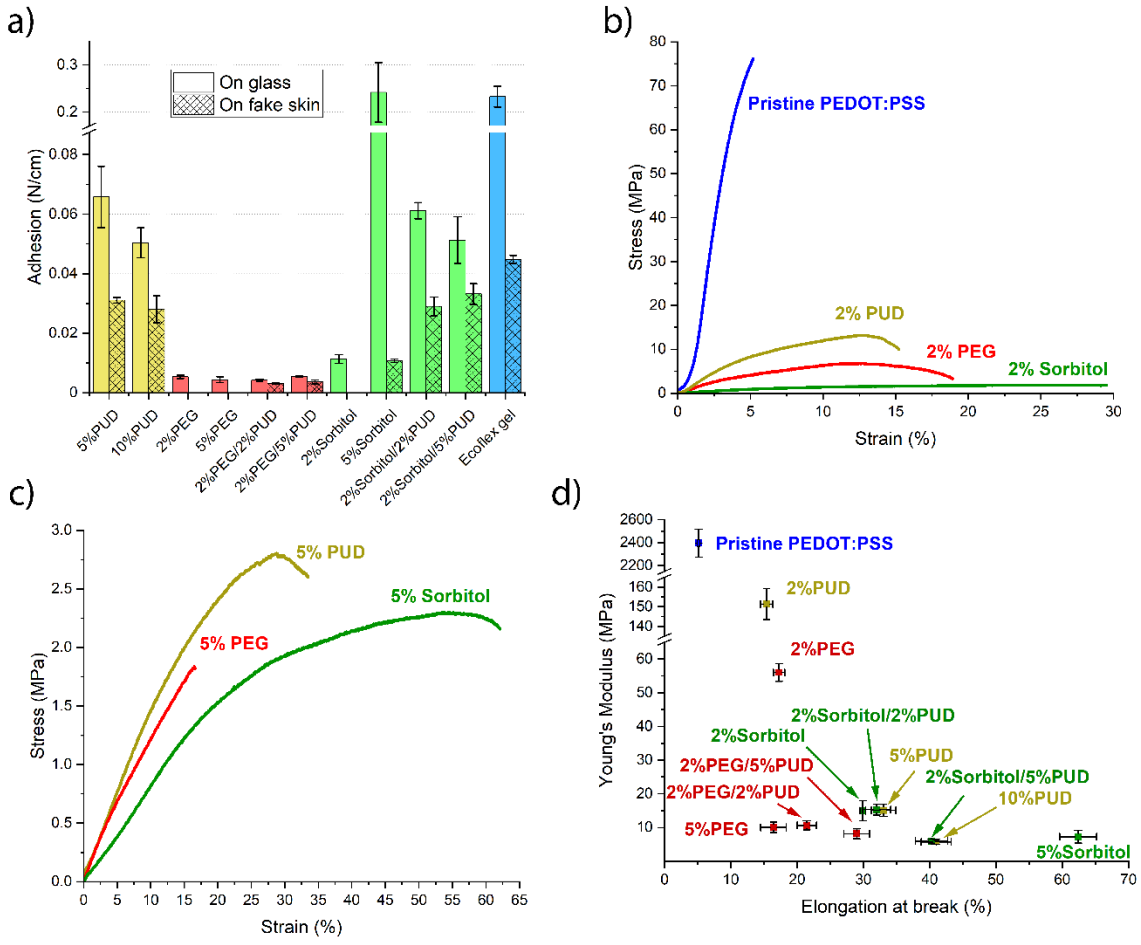

Figure 4.2 a) Adhesion on glass and on fake skin for different compositions of PEDOT:PSS based films and the Ecoflex gel (n = 3). Strain-stress curves of PEDOT:PSS with b) low percentage additives (pristine PEDOT:PSS, 2% PUD, 2% PEG and 2% sorbitol) and c) 5% PUD, 5% PEG and 5% sorbitol. d) Relationship between Young's modulus and elongation at break for different compositions of PEDOT:PSS based films (n = 3).

To facilitate painless removal of the electrodes from the skin, we targeted an adhesion comparable to that of Ecoflex [85, 109], which showed an average adhesion force of 0.045 N/cm on fake skin (Figure 4.2a and Table S2). Painless removal of adhesive was observed in clinical research for up to ~0.5 N/cm [125, 126]. The pristine PEDOT:PSS and the 2% PUD/PEDOT:PSS

films did not adhere on glass or on fake skin. The 5% PUD/PEDOT:PSS, 10% PUD/PEDOT:PSS, 2% sorbitol/2%PUD/PEDOT:PSS, and 2%PUD/5%sorbitol/PEDOT:PSS films demonstrated an adhesion on fake skin similar to that of the Ecoflex gel (Figure 4.2a).This indicates that adding enough PUD and sorbitol improves the film's adhesion. However, as 10% PUD/PEDOT:PSS films had a viscous residue on their surface after drying due to excess PUD, they were not considered suitable for epidermal electrodes. While the addition of PEG significantly improved the conductivity, the films exhibited a weak adhesion on both glass and fake skin making them unsuitable for adhesive epidermal electrodes.

Stretchability and a Young's modulus similar to that of the skin are crucial characteristics for epidermal electrodes, to maintain proper contact with the skin, prevent irritation, and ensure the wearer's comfort [127]. The Young's modulus of human skin can range from 5 kPa to 140 MPa (depending on whether it is measured by indentation in the thickness-direction for lower modulus or by tensile test for higher modulus) [128]. Therefore, we studied the mechanical properties of the films with different compositions. The strain-stress curves in Figure 4.2b refer to films made of pristine PEDOT:PSS and its mixtures with 2% of PUD, PEG, or sorbitol. Figure 4.2c depicts the strain-stress curves for PEDOT:PSS films with 5% of PUD, PEG and sorbitol.

Our results unequivocally show that adding PUD, PEG and sorbitol to PEDOT:PSS leads to films with larger elongations at break and lower Young's moduli when compared to pristine PEDOT:PSS (Figure 4.2d, Table S 3). The most stretchable films (up to 66%) were obtained from 10% PUD/PEDOT:PSS, 5% sorbitol/PEDOT:PSS, and 2% sorbitol/5% PUD/PEDOT:PSS. The incorporation of sorbitol had the most significant effect on the stretchability of PEDOT:PSS films. Adding PUD to sorbitol/PEDOT:PSS further improved the film's stretchability. Increasing the amount of PEG was effective in reducing the material's Young's modulus and increasing its conductivity, but the elongation remained almost identical for samples with 2% and 5% PEG. However, a significant improvement in stretchability was observed when adding 5% PUD to 2% PEG films. This effect can be attributed to the formation of hydrogen bonds between the additives and PSS, which decrease the interactions between PEDOT and PSS chains and leads to an increase of the free volume between polymer chains [1, 45]. The ensuing chain separation and uncoiling of PEDOT:PSS reduces the distance between conductive PEDOT chains, thereby

improving the conductivity of the resulting polymer blend [129, 130]. We hypothesize that water-soluble PUD exerts comparable effects on improving film stretchability and conductivity.

4.3.3 Electrical characterization

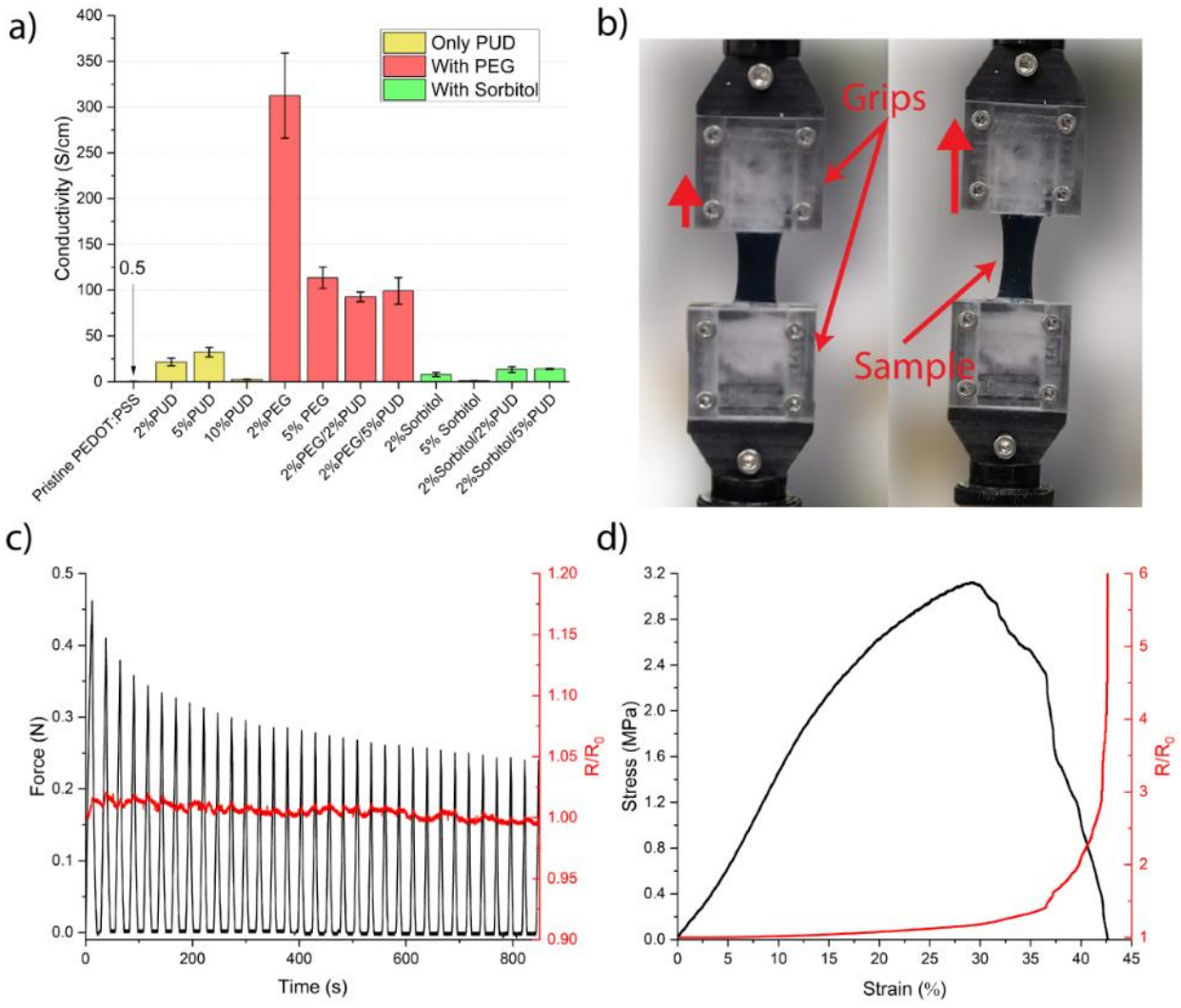

Figure 4.3 a) Conductivity of films based on different formulations of PEDOT:PSS. (n = 3) b) Photo of the electromechanical measurement setup with grips, sample, and direction of stretching identified. c) Resistance variation vs time of 5% PUD/PEDOT:PSS film when cyclically stretched 10% of initial length. d) Resistance change of a 5% PUD/PEDOT:PSS film when stretched until break.

We subsequently investigated the electrical properties of the different films. The pristine PEDOT:PSS film exhibited an average conductivity of around 0.5 S/cm, which increased upon the addition of low percentages of plasticizers (Figure 4.3a, Table S 3). The 2%

PEG/PEDOT:PSS demonstrated the highest conductivity with an average of about 300 S/cm, consistent with previously reported data for PEDOT:PSS film with 1% PEG [49]. Incorporation of 2% sorbitol yielded an average conductivity of about 8 S/cm while increasing to 5% sorbitol decreased the conductivity to around 1 S/cm. Whereas 5% PUD/PEDOT:PSS resulted in an average conductivity of about 30 S/cm, increasing the PUD content to 10% decreased the conductivity to around 2.5 S/cm. Blending 2% PEG with 5% PUD increased the conductivity to approximately 100 S/cm and simultaneously improved the stretchability when compared to 2% PEG alone. Nonetheless, after a certain amount of additives is incorporated to PEDOT:PSS, the electrical conductivity decreases. Among the selected additives, sorbitol led to the smallest conductivity enhancement. This may be attributed to the low heating temperature (70°C) used during the film preparation [48]. After annealing the sorbitol/PUD/PEDOT:PSS films at 160°C for 15 seconds on a hotplate, a significant improvement of the conductivity was observed (Table S 4). However, this process led to a decline in the films' stretchability and adhesion, rendering them unsuitable for epidermal electrodes. As a result, 70°C was selected as the optimal temperature to remove the water and obtain the films.

In a further attempt to assess the stability of PEDOTPSS-based films over time, three types of samples (5% PUD/PEDOT:PSS, 5% PEG/PEDOT:PSS, and 5% sorbitol/PEDOT:PSS) were stored under ambient conditions for a week, and then their mechanical properties were characterized (Table S 5). We observed that the mechanical properties of 5% PEG/PEDOT:PSS films remained virtually unchanged. 5% PUD/PEDOT:PSS films exhibited ~55% increase in their Young's modulus and ~30% decrease in elongation at break. The 5% sorbitol/PEDOT:PSS films demonstrated the most significant deterioration, becoming brittle, with its Young's modulus increasing more than 20-fold and a drastic reduction in elongation at break to only 10% of its original value. These alterations can likely be traced back to the loss of additives and slow water evaporation following the initial heating step. Finally, to evaluate their resilience when exposed to water or sweat, these samples were submerged in water. The 5% sorbitol/PEDOT:PSS film completely dissolved, while the PEDOT:PSS films containing 5% PUD and 5% PEG remained undamaged (Figure S 5).

Considering their adhesion, mechanical and electrical properties, 5% PUD/PEDOT:PSS films emerge as the most promising candidates for fabricating epidermal electrodes. They exhibited superior conductivity than films with sorbitol and enhanced elongation compared to PEG films. Consequently, we selected these films for electromechanical testing. To characterize the electrical stability under mechanical strain, we subjected the 5% PUD/PEDOT:PSS films to a series of cyclic strains - up to 10% of their initial length - to remain within the material's elastic domain. The film demonstrated excellent stability under repeated stretching, with a resistance variation below 2%, as evidenced in Figure 4.3c. Furthermore, the resistance's change with uniaxial deformation is shown in Figure 4.3d. The resistance rose by less than 20% before the onset of breaking, after which it escalated by over 100% when the film started breaking around 30% strain mark (Figure 4.3d). These findings substantiate the excellent electrical stability of PUD/PEDOT:PSS films under moderate strains, suggesting they can mimic skin's stretchability without notably compromising the electrode's conductivity.

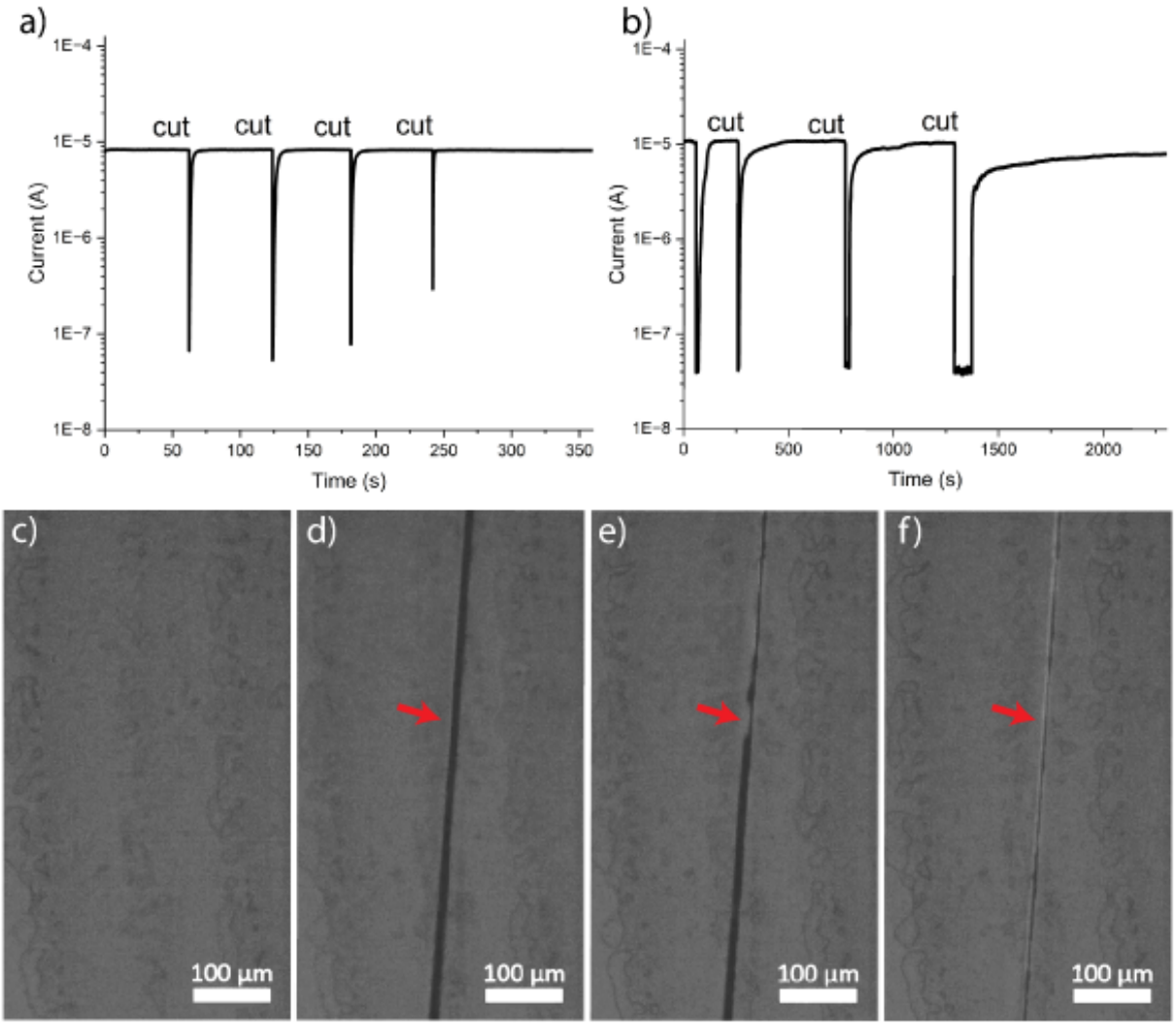

Figure 4.4 Current vs time plot showing repeated electrically self-healing of a) drop-cast and b) printed 5% PUD/PEDOT:PSS films for four cuts at different locations. Optical microscopic images of a 5% PUD/PEDOT:PSS free-standing film on glass c) before damage, d) after cutting with a razor blade, e) partially healed, and f) fully healed approximately 5 seconds after the cut.

Furthermore, ideal materials for wearable electronics should be resilient to physical damage and possess the capacity to mend minor cracks when subjected to mechanical injuries, such as cuts. In an effort to evaluate whether our PEDOT:PSS-based films exhibit this property, a 5% PUD/PEDOT:PSS free-standing film was completely cut using a razor blade while monitoring the current under constant voltage. As depicted in Figure 4.4a, upon the complete separation of

the film, the current dropped to the noise level, indicative of interrupted electrical conduction. Immediately after the cut, the two parts autonomously came into contact, leveraging the intrinsic self-healing nature of the PUD/PEDOT:PSS film (Movie S1), and the current was restored to ~100% of its initial level. We executed this process several times on the same film and consistently witnessed this behavior.

The self-healing ability of 5% PEG/PEDOT:PSS and 5% sorbitol/PEDOT:PSS films were also examined (Figure S 6). The free-standing 5% PEG/PEDOT:PSS film showed no significant decrease in current when cut, but the current was noisier than the other types of samples. Although the 5% sorbitol/PEDOT:PSS film nearly fully recovered after the initial two cuts, subsequent cuts led to only partial recovery. Thus, 5% PUD/PEDOT:PSS film demonstrated superior electrical self-healing behavior compared to its counterparts. The same test was performed on a printed 5% PUD/PEDOT:PSS film which also revealed consistent electrical self-healing (Figure 4.4b). This recurrent self-healing ability aligns with findings from other studies examining PEDOT:PSS-based self-healable materials with other additives [49, 115, 131]. Due to the manual nature of the cuts, individual variations may account for slower and reduced current recovery after the 4^{th} cut on the printed sample. Figure 4.4c-f provide the microscope images of the 5% PUD/PEDOT:PSS film prior to and post damage, as well as during its recovery.

The integration of plasticizers or other polymers, such as PUD, into PEDOT:PSS leads to electrical self-healing, achieved through reduced polymer film crystallinity, increased viscoelasticity, and decreased Young's moduli [131]. Furthermore, π-π interactions between PEDOT:PSS's aromatic groups, and hydrogen bonds between urethane groups on PUD and sulfonate groups on PSS, likely bolster the self-healing ability of PUD/PEDOT:PSS composite [131]. Owing to its high electrical conductivity, suitable stretchability, adequate adhesion, and consistent electrical self-healing behavior, we have selected 5% PUD/PEDOT:PSS for fabricating the epidermal electrodes.

4.3.4 Physico-chemical characterization

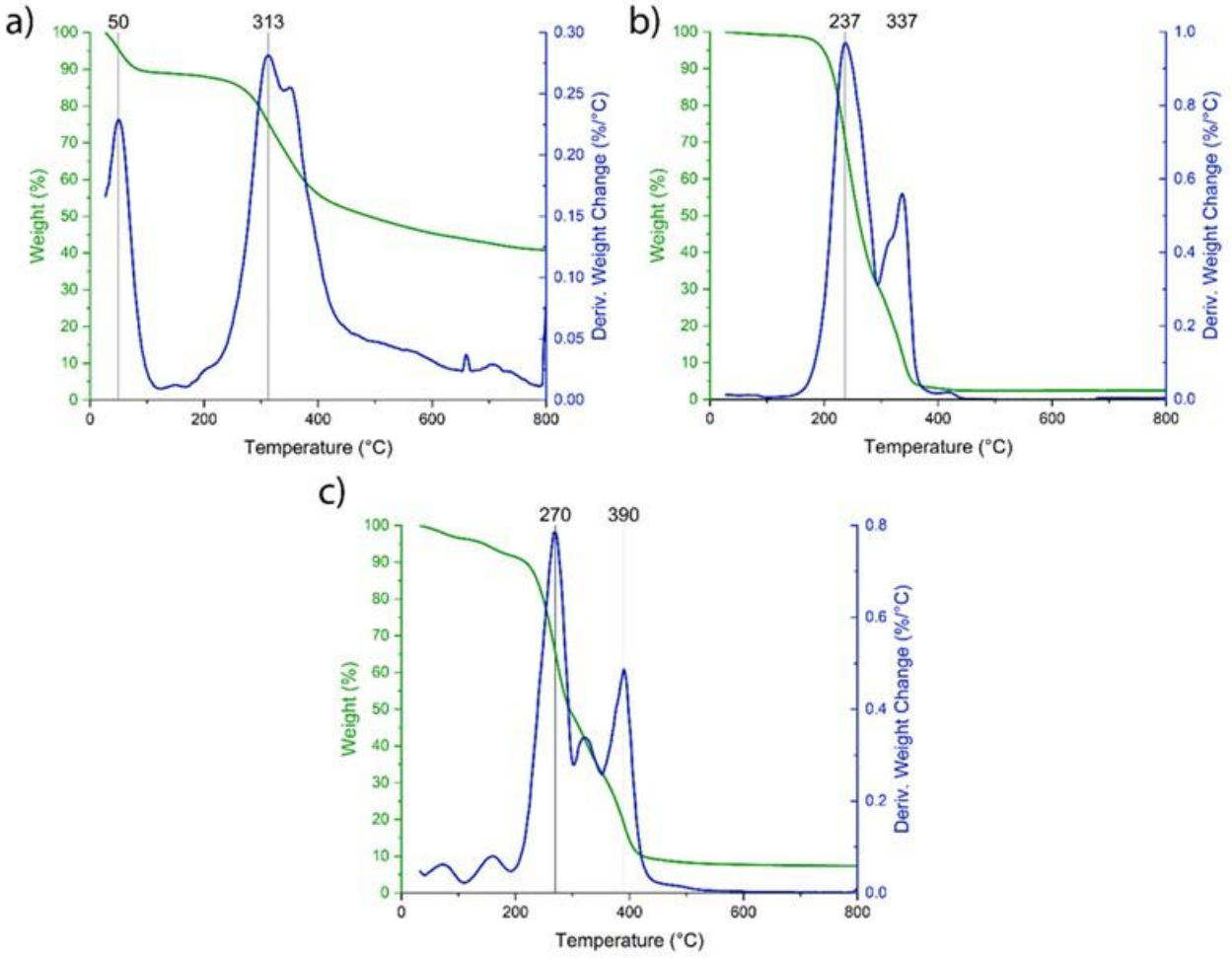

Figure 4.5 Thermogravimetry (TGA) and derivative thermogravimetry (DTG) curves of dried a) pristine PEDOT:PSS, b) pristine PUD, and c) PEDOT:PSS with 5% PUD.

Since the 5% PUD/PEDOT:PSS demonstrated the most appealing properties for epidermal electrodes, we conducted both TGA and FTIR measurements on pristine PEDOT:PSS, pristine PUD, and a 5% PUD/PEDOT:PSS film. These tests allowed us to confirm the enduring presence of PUD in the film post-processing, investigate the film's water content, and delve deeper into the interaction between PEDOT:PSS and PUD.

The pristine PEDOT:PSS film contained about 10 wt% of water, as approximately 10% weight reduction was observed when the sample was heated to 100°C (Figure 4.5a). Conversely, the

fully dried PUD sample revealed no residual water (Figure 4.5b). As illustrated in Figure 4.5c, the 5% PUD/PEDOT:PSS sample contains about 5% of water, qualifying it as a dry electrode.

Due to its low water content, especially when compared to wet electrodes such as hydrogel-based alternatives, dry electrodes tend to be more durable over time as their functionality remains unaffected by water loss. Hydrogel-based epidermal electrodes suffer from water evaporation at room temperature in a short period of time, leading to reduced signal recording quality and increased impedance at the skin-electrode interface. As such, low water content is a definite advantage for long-term use of functional epidermal electrodes. The modest water content in PEDOT:PSS-based films can be attributed to the moisture retention ability inherent in PEDOT:PSS [132].

Furthermore, the DTG peaks for the 5% PUD/PEDOT:PSS film moved towards higher temperatures compared to pristine PEDOT:PSS and pristine PUD samples. This shift provides qualitative support for the presence of hydrogen bonds [133] between PEDOT:PSS and PUD. For pristine PEDOT:PSS, the pyrolysis peak resides around 313°C (Figure 4.5a), whereas there are two peaks for pristine PUD, one at 237°C and the second at 337°C (Figure 4.5b).

The thermal degradation of the 5% PUD/PEDOT:PSS mirrored the pristine PUD, occurring in two pyrolysis stages. However, unlike the pristine PUD sample, a shift towards higher pyrolysis temperatures at 270°C and 390°C was measured (Figure 4.5c). The DTG curves of 2% sorbitol/5% PUD/PEDOT:PSS and 2%PEG/5% PUD/PEDOT:PSS also exhibited a shift towards higher pyrolysis temperatures (Figure S 7a,b) when compared to the pristine PEDOT:PSS and PUD samples.

Figure S 8a displays the FTIR spectra for pristine PEDOT:PSS, pristine PUD, and 5% PUD/PEDOT:PSS, while the FTIR spectra for PEDOT:PSS samples containing PUD, PEG and sorbitol are shown in Figure S 8b. For pristine PUD and 5% PUD/PEDOT:PSS samples, the characteristic peaks are observed at 3318 cm^{-1} for -NH stretching of urethane component in PUD, 2933 cm^{-1} for -CH stretching of alkanes in PUD, and 1684 cm^{-1} for C=O stretching of the urethane component. These observations confirm the presence of PUD in the final 5%PUD/PEDOT:PSS film.

4.3.5 Biocompatibility

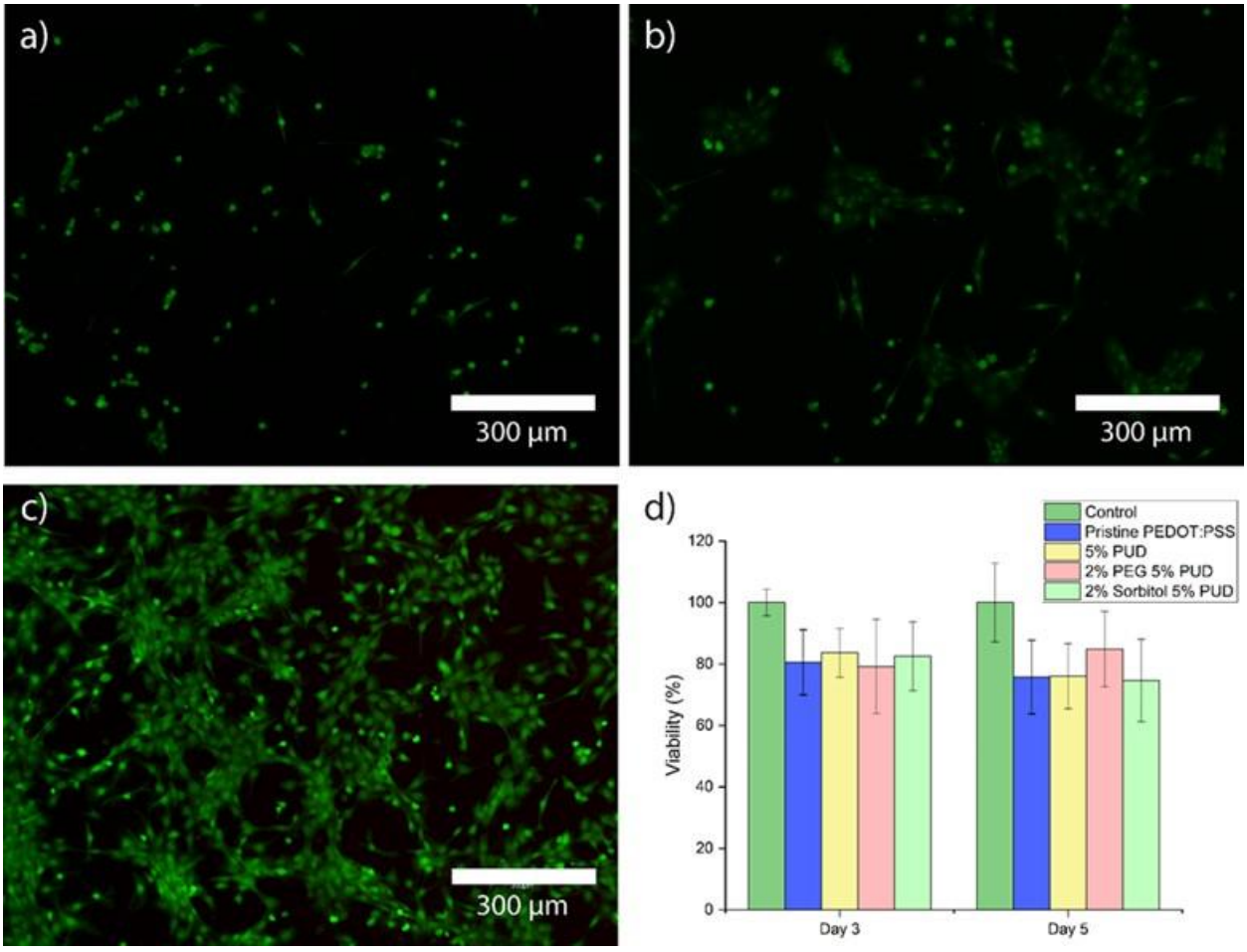

Figure 4.6. Seeded C2C12 cells on 5% PUD/PEDOT:PSS coating after a) 1 day, b) 3 days, and c) 5 days. Scale bar is 300 µm. d) Viability of cells on pristine PEDOT:PSS, 5% PUD/PEDOT: PSS, 2% PEG/5% PUD/PEDOT:PSS, and 2% sorbitol/5% PUD/PEDOT:PSS compared to the control collected on day 3 and 5 (n = 3).

To assess the biocompatibility of our PEODT:PSS formulations, C2C12 rat muscle cells were attached and cultured on thin coatings of 5% PUD/PEDOT:PSS. The cells were stained with calcein AM to show intracellular esterases activity for live cells with green fluorescence and EthD-1 for dead or dying cells with damaged membranes as red fluorescence. After one day of

culture, some cells seemed attached to the surface, adopting a flattened shape, while others were still round and not fully attached (Figure 4.6a). After 3 days, the majority of the cells had adhered, and the population had expanded (Figure 4.6b). By day-5, the cells had achieved confluency with only a few showing signs of apoptosis (Figure 4.6c). The viability of cells for day 3 and 5 was confirmed using fluorescence measurements through a microplate reader. These results were compared to uncoated polystyrene wells serving as positive control (Figure 4.6d). As there is no significant difference between pristine PEDOT:PSS and PEDOT:PSS with 5%PUD, we can conclude that PUD does not significantly affect the viability. From observations during the cell culture, the ~20% decrease between the positive control and the tested samples might be attributed to the decreased adhesion of cells on PEDOT:PSS and their slower growth. The cell viability could potentially be increased by first allowing the cells to freely adhere to the uncoated surface, and subsequently add the tested mixture and observe the growth of cells. In accordance with ISO10993-5, as the average relative viability for PEDOT:PSS films containing PUD is higher than 70% of the control group, they are considered non-cytotoxic [134]. Moreover, the viability of PEDOT:PSS with 5% PUD does not significantly deviate from PEDOT:PSS alone or when combined with PEG or sorbitol. Hence, the addition of up to 5% PUD does not impact the biocompatibility of PEDOT:PSS films.

4.3.6 Electrophysiological measurements

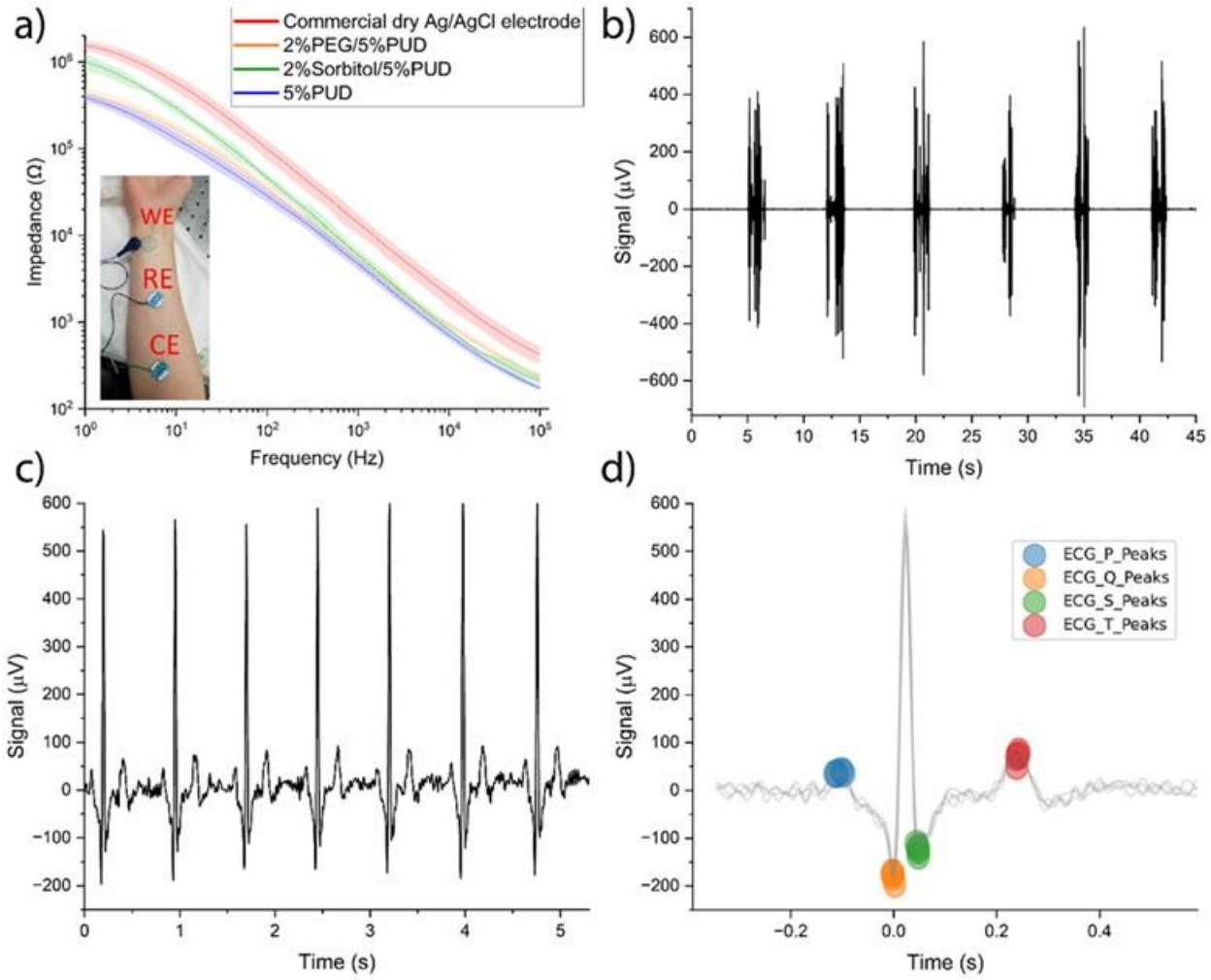

Figure 4.7. a) Skin-electrode impedance of commercial electrode and PEDOT:PSS based electrodes with 2% PEG/5% PUD, 2% sorbitol/5% PUD, and 5% PUD (n = 3), and photo of the impedance measurement configuration with working (WE), reference (RE) and counter (CE) electrodes identified (inset). The shaded area around each curve represents their respective standard deviations. b) Electromyogram (EMG) for biceps muscle and c) electrocardiogram (ECG) signals measured using printed 5% PUD/PEDOT:PSS electrodes. d) Delineated ECG complexes from previous graph with identifiable relevant peaks.

We next examined the performance of 5% PUD/PEDOT:PSS films printed on Ecoflex gel/PDMS substrate as epidermal electrodes for electrophysiological signal collection. The measurement setup is shown in the inset of Figure 4.7a. Skin-electrode impedance measurements revealed that printed 5% PUD/PEDOT:PSS electrodes on Ecoflex substrate had slightly lower impedance, exhibiting comparable performance to commercial electrodes (Figure 4.7a). Nonetheless, it should be noted that skin-electrode impedance measurements can differ greatly depending on the person and ambient conditions such as temperature and humidity. Using the 5% PUD/PEDOT:PSS epidermal electrodes, electromyogram (Figure 4.7b) and electrocardiogram (Figure 4.7c) signals were recorded with recognizable ECG peaks (Figure 4.7d). The properties of our printed 5% PUD/PEDOT:PSS based skin electrode are listed in Table 2 alongside other electrodes reported in literature. When contrasted with inkjet-printed PEDOT:PSS electrode on paper[135], our PUD/PEDOT:PSS electrode has superior stretchability and lower skin-electrode impedance, despite exhibiting lower conductivity. This improvement is likely due to the electrode's adhesion creating a tighter interface with the skin, thereby eliminating air gaps at the contact region, unlike dry non-adhesive electrodes. PEDOT:PSS electrodes combined with waterborne PU and sorbitol display high electrical conductivity and low skin-electrode impedance [58]. Our PUD/PEDOT:PSS electrodes are printable and have lower Young's modulus, which may be due PUD's lower molecular weight compared to waterborne PU.

Table 3. Reported epidermal electrode materials and properties including Young's modulus, electrical conductivity, skin-electrode impedance, adhesion, and printability.

Fabrication Method	Material	Modulus (MPa)	Conductivity ($S \cdot cm^{-1}$)	Skin-electrode impedance at 10 Hz ($k\Omega \cdot cm^2$)	Adhesion	Ref
Microfabrication	PDMS, silver microparticles	1	>100	50	Yes	[85]
Inkjet printing	PEDOT:PSS (PH1000) on paper	N/A	~240	3680 (1 Hz)	No	[135]
Molding	PEDOT:PSS (PH1000), waterborne PU, sorbitol	~40	~350	80	Yes	[58]
Screen-printing	PEDOT:PSS (PH1000), DMSO, Triton X-100 with Cetaphil lotion, on textile	N/A	N/A	270	No	[136]
Direct-ink write printing	5% PUD/PEDOT:PSS (PH1000), silver, on PDMS/Ecoflex	15	32	370 (10 Hz) 1111	Yes	This work

(1 Hz)

4.4 Conclusions

In summary, we investigated and presented a printable PEDOT:PSS-based formulation characterized by light adhesion, stretchability, high conductivity, and electrical self-healing ability. As a result of studying the effects of different additives, a light adhesion of ~0.03 N/cm was obtained for the 5% PUD/PEDOT:PSS films with a conductivity of approximately 30 S/cm and a stretchability of 30%, stemming from PUD. Moreover, PUD/PEDOT:PSS films demonstrated resilience to repeated strains, consistent electrical self-healing, and biocompatibility. These are critical properties for durable and reliable epidermal electrodes. Finally, to demonstrate the potential for soft electronics, we fabricated PUD/PEDOT:PSS dry electrodes using direct-ink writing. The electrodes displayed similar skin-electrode impedance as commercial Ag/AgCl dry gel electrodes and successfully recorded ECG and EMG signals. Long term electrophysiological recordings are crucial for hospitalized patients requiring constant monitoring. The dry electrodes developed in this work feature tunable adhesion and do not apply a strong peel-off force on the skin when removed, making them suitable for continuous recordings. In addition, the PUD/PEDOT:PSS dry electrodes do not suffer from water loss like conventional hydrogel-based electrodes. Therefore, these printable dry electrodes hold promising potential for healthcare monitoring. Since the PEDOT:PSS formulation is printable, this research paves the way for the development of rapid customizable dry self-healable electrodes with tunable adhesion, electrical, and mechanical properties. Further research needs to be conducted to achieve reusable adhesives and tests for prolonged monitoring of electrophysiological signals on patients with sensitive skin such as premature infants.

CRediT authorship contribution statement

Pierre Kateb: Conceptualization, Methodology, Validation, Formal analysis, Investigation, Visualization and Writing – original draft. **Jiaxin Fan:** Analysis, Writing – review and editing. **Jinsil Kim**: Investigation, Writing – review and editing. **Xin Zhou**: Analysis, Writing – review and editing. **Gregory Lodygensky**: Writing – review and editing, Supervision. **Fabio Cicoira**: Writing – review and editing, Supervision.

Declaration of Competing Interest

The authors declare that they have no known competing financial interests or personal relationships that could have appeared to influence the work reported in this paper.

Data availability

The data supporting the findings of the study are available upon request.

Funding

This work was supported by the Natural Sciences and Engineering Research Council of Canada (NSERC), the *Fonds de recherche du Québec – Nature et technologies* (FRQNT, 316968), and the Pierre Arbour foundation. Additional funding is provided by Transmedtech Institute and Canada First Research Excellence Fund through the project *Stretchy Electrodes*. Equipment and infrastructure used for this research were acquired and maintained by the Canada Foundation for Innovation and Quebec Strategic Networks (RQMP and CREPEC).

Ethical statement

The protocol for human experiments was approved by the ethical committee of Polytechnique Montreal (approval number CER-2021-04-D).

CHAPTER 5 GENERAL DISCUSSION

Stretchable, adhesive, and self-healing materials are promising candidates for epidermal electrodes due to their superior skin-electrode contact. To surpass the limitations of conventional wet electrodes, various materials such as hydrogel and organohydrogels, and dry electrodes such as fabric-based [80] electrodes and glueless adhesive [85, 108] electrodes have been researched. Nonetheless, fabrication of suitable electrodes for premature infants presents a persistent challenge.

Furthermore, there is a lack of studies testing and quantifying the appropriate adhesion levels of epidermal electrodes on premature skin. An adhesion of ~0.5 N/cm was quantified for pain tolerance in adults [125, 126], however it is expected to be lower in premature infants. This kind of study would help better fine-tune de adhesion our electrodes with adhesive additives we used or that have been reported in literature such as polydopamine [137, 138], tannic acid [139, 140], or acrylic adhesives, as well as their combinations. In addition, the nature of additives might have diverse effects on premature infants [105] compared to newborns or adult, due to the thinner skin-barrier of premature infants. It is therefore critical to evaluate new epidermal electrodes materials across different compatibility stages, as a standard biocompatibility test on cells of the materials used for epidermal electrodes does not fully represent the potential effect of these materials on real human tissue and surrounding organs.

The incorporation of additives such as sorbitol, PEG, and PUD as plasticizers also showed promise for tailoring the electrical, mechanical, adhesive, and self-healing properties of materials. A significant opportunity lies in their combination. For instance, we found that blending PUD and PEG in PEDOT:PSS resulted in films with more stretchability than PEG alone, while exhibiting higher conductivity than PEDOT:PSS films with PUD alone.

Moreover, the investigation of properties for durable materials such as self-healing ability, forms an integral part of the research conducted. Given the best-case scenario for developing epidermal electrodes which would need to be suitable for long-term use, water-based electrodes were immediately disregarded from the beginning. Similarly, the use of sorbitol was eliminated from consideration due to its notable degradation in mechanical properties over a short period of time under ambient conditions.

The development of stretchable, adhesive, and self-healing epidermal electrodes for preterm infants has significant challenges. Notable advancements have been made using conductive polymers, particularly PEDOT:PSS for epidermal applications, with a significant emphasis on material design, notably through the incorporation of additives to fine-tune its various properties.

CHAPTER 6 CONCLUSION AND RECOMMENDATIONS

This thesis explored a fabrication method to obtain printable and stretchable dry epidermal electrodes able to achieve conformal contact with the skin without exerting a strong adhesion. Extensive research has already been conducted on epidermal electrodes. On one hand, wet electrodes, traditionally employing electrolytes as ionic conductors, offer a good interface between the skin and the electrode. Nevertheless, they have a notable disadvantage due to inadequacy for long term use due to their water content which evaporates over time. A prospective solution to this issue lies in organohydrogels, which replace water with less volatile solvents such as glycerol, thereby addressing the problem of water loss.

On the other hand, dry electrodes would bypass the issue with solvents. Subsequently, the exploration of dry adhesive electrodes featuring tunable adhesion presents a crucial area of study to further improve epidermal electrodes, specifically considering the unique needs of premature skin. Given the vulnerability of preterm skin, we identified a necessity to develop adhesive solutions that avoid the risks of medical-adhesive related skin injuries and ensure high-quality measurements.

In addition, the incorporation of conductive polymers, notably PEDOT:PSS, known for its excellent processability, biocompatibility, adaptability to soft tissues, and ability to lower skin-electrode impedance, can significantly improve the performance of these electrodes.

This study demonstrated the development and characterization of a printable, stretchable, lightly adhesive, and self-healing dry material suitable for biomedical applications. This research explored the use of plasticizers such as polyurethane diol (PUD), polyethylene glycol (PEG), and sorbitol as additives to PEDOT:PSS to further enhance the mechanical properties, notably stretchability and adhesion, and electrical properties of PEDOT:PSS, leading to an optimized printable mixture. This combination allowed the material to improve its conductivity and stretchability. It also exhibits light adhesion, making it an ideal candidate for epidermal applications for people with sensitive skin such as preterm infants.

Regarding processing of PEDOT:PSS, printing technologies offer various opportunities for the fabrication of epidermal electrodes. This work showed the direct-write printing of a composite

ink, which offers easy and inexpensive customization, facilitating the creation of electrodes, and rapid prototyping. Moreover, self-healing printed electronics are particularly promising. By combining the resilience of self-healing materials with the customization and scalability offered by printability, we can produce durable and reliable electronic devices with the capability to recover from damage and extend their lifespan. Conductive polymers like PEDOT:PSS, particularly when fine-tuned with plasticizers, are promising in this context. Through the addition of PUD to PEDOT:PSS printable self-healing electrodes were fabricated. Conductive, printable, self-healing, adhesive and stretchable electrodes hold tremendous potential for wearable and epidermal electronic systems and should be further researched in future works.

Finally, with the recording of electrophysiological signs in mind, an interesting yet unexplored prospect in the scope of this work is the use of OECTs as epidermal electrodes. Owing to their ability to amplify signals, they could help collecting smaller signals such as those from EEG.

Additionally, to improve the mechanical properties of electrodes, metamaterials present a promising approach as they do not rely on the intrinsic properties of the material but modify its structure to enhance its properties. Metamaterials such as auxetic structures could significantly improve the stretchability of electrodes built on stiffer materials. Similarly, as previously reported for microstructures inspired from the feet of insects, surface structure modifications could serve as a promising strategy to tune the adhesion of electrodes on different types of skins.

REFERENCES

[1] L.-W. Lo, J. Zhao, H. Wan, Y. Wang, S. Chakrabartty, and C. Wang, "An inkjet-printed PEDOT: PSS-based stretchable conductor for wearable health monitoring device applications," *ACS Applied Materials & Interfaces,* vol. 13, no. 18, pp. 21693-21702, 2021.

[2] Y. J. Hong, H. Jeong, K. W. Cho, N. Lu, and D. H. Kim, "Wearable and implantable devices for cardiovascular healthcare: from monitoring to therapy based on flexible and stretchable electronics," *Advanced Functional Materials,* vol. 29, no. 19, p. 1808247, 2019.

[3] C. Binnie and P. Prior, "Electroencephalography," *Journal of Neurology, Neurosurgery & Psychiatry,* vol. 57, no. 11, pp. 1308-1319, 1994.

[4] K. R. Mills, "The basics of electromyography," *Journal of Neurology, Neurosurgery & Psychiatry,* vol. 76, no. suppl 2, pp. ii32-ii35, 2005.

[5] C. Tronstad, M. Amini, D. R. Bach, and O. G. Martinsen, "Current trends and opportunities in the methodology of electrodermal activity measurement," *Physiological Measurement,* 2022.

[6] S. R. Gutbrod, M. S. Sulkin, J. A. Rogers, and I. R. Efimov, "Patient-specific flexible and stretchable devices for cardiac diagnostics and therapy," *Progress in biophysics and molecular biology,* vol. 115, no. 2-3, pp. 244-251, 2014.

[7] D. Xie *et al.*, "Identification of an endogenous glutamatergic transmitter system controlling excitability and conductivity of atrial cardiomyocytes," *Cell Research,* vol. 31, no. 9, pp. 951-964, 2021.

[8] N. A. Campbell, J. B. Reece, L. Urry, M. Cain, S. Wasserman, and P. Minorsky, "Biology. ed," ed: San, Francisco: Pearson Benjamin Cummings, 2008.

[9] B. Alberts *et al.*, *Essential cell biology*. Garland Science, 2015.

[10] S. B. Rutkove, "Introduction to volume conduction," *The clinical neurophysiology primer,* pp. 43-53, 2007.

[11] D. Dumitru and J. A. Delisa, "AAEM Minimonograph# 10: volume conduction," *Muscle & Nerve: Official Journal of the American Association of Electrodiagnostic Medicine,* vol. 14, no. 7, pp. 605-624, 1991.

[12] G. Buzsáki, C. A. Anastassiou, and C. Koch, "The origin of extracellular fields and currents—EEG, ECoG, LFP and spikes," *Nature reviews neuroscience,* vol. 13, no. 6, pp. 407-420, 2012.

[13] F. L. Da Silva, "EEG: origin and measurement," in *EEG-fMRI: physiological basis, technique, and applications*: Springer, 2023, pp. 23-48.

[14] M. J. Christie, "Electrodermal Activity in the 1980s: A Review," *Journal of the Royal Society of Medicine,* vol. 74, no. 8, pp. 616-622, 1981, doi: 10.1177/014107688107400812.

[15] B. Cornish, B. Thomas, and L. Ward, "Effect of temperature and sweating on bioimpedance measurements," *Applied Radiation and Isotopes,* vol. 49, no. 5-6, pp. 475-476, 1998.

[16] G. Petrossian, P. Kateb, F. Miquet-Westphal, and F. Cicoira, "Advances in Electrode Materials for Scalp, Forehead, and Ear EEG: A Mini-Review," *ACS Applied Bio Materials,* 2023/07/26 2023, doi: 10.1021/acsabm.3c00322.

[17] H. Yuk, B. Lu, and X. Zhao, "Hydrogel bioelectronics," *Chemical Society Reviews,* vol. 48, no. 6, pp. 1642-1667, 2019.

[18] S. Lin *et al.*, "Stretchable hydrogel electronics and devices," *Advanced Materials,* vol. 28, no. 22, pp. 4497-4505, 2016.

[19] X. Zhou *et al.*, "Self-healing, stretchable, and highly adhesive hydrogels for epidermal patch electrodes," *Acta Biomaterialia,* vol. 139, pp. 296-306, 2022.

[20] A. Searle and L. Kirkup, "A direct comparison of wet, dry and insulating bioelectric recording electrodes," *Physiological measurement,* vol. 21, no. 2, p. 271, 2000.

[21] N. Meziane, J. Webster, M. Attari, and A. Nimunkar, "Dry electrodes for electrocardiography," *Physiological measurement,* vol. 34, no. 9, p. R47, 2013.

[22] H. Shirakawa, "The discovery of polyacetylene film: the dawning of an era of conducting polymers (Nobel lecture)," *Angewandte Chemie International Edition,* vol. 40, no. 14, pp. 2574-2580, 2001.

[23] H. Shirakawa, E. J. Louis, A. G. MacDiarmid, C. K. Chiang, and A. J. Heeger, "Synthesis of electrically conducting organic polymers: halogen derivatives of polyacetylene,(CH) x," *Journal of the Chemical Society, Chemical Communications,* no. 16, pp. 578-580, 1977.

[24] J. Casselman, N. Onopa, and L. Khansa, "Wearable healthcare: Lessons from the past and a peek into the future," *Telematics and Informatics,* vol. 34, no. 7, pp. 1011-1023, 2017.

[25] J. Mutifa, N. Nurhaeni, and D. Wanda, "The Effectiveness Of The Protective Barrier Of The Skin Against Medical Adhesive Related Skin Injury (Marsi) In Children Treated In Pediatric Intensive Care Units: Systematic Review," *Jurnal Keperawatan Komprehensif (Comprehensive Nursing Journal),* vol. 8, no. Special Edition, 2022.

[26] D. Wang, H. Xu, S. Chen, X. Lou, J. Tan, and Y. Xu, "Medical adhesive-related skin injuries and associated risk factors in a pediatric intensive care unit," *Advances in skin & wound care,* vol. 32, no. 4, pp. 176-182, 2019.

[27] J. Werth, L. Atallah, P. Andriessen, X. Long, E. Zwartkruis-Pelgrim, and R. M. Aarts, "Unobtrusive sleep state measurements in preterm infants–A review," *Sleep medicine reviews,* vol. 32, pp. 109-122, 2017.

[28] V. K. Varadan, "Nanosensors, Biosensors, Info-Tech Sensors and 3D Systems 2017," in *Society of Photo-Optical Instrumentation Engineers (SPIE) Conference Series*, 2017, vol. 10167.

[29] J. Rivnay *et al.*, "Structural control of mixed ionic and electronic transport in conducting polymers," *Nature Communications,* vol. 7, no. 1, p. 11287, 2016/04/19 2016, doi: 10.1038/ncomms11287.

[30] M. J. Donahue *et al.*, "Tailoring PEDOT properties for applications in bioelectronics," *Materials Science and Engineering: R: Reports,* vol. 140, p. 100546, 2020.

[31] T. Someya, Z. Bao, and G. G. Malliaras, "The rise of plastic bioelectronics," *Nature,* vol. 540, no. 7633, pp. 379-385, 2016.

[32] R. Balint, N. J. Cassidy, and S. H. Cartmell, "Conductive polymers: Towards a smart biomaterial for tissue engineering," *Acta biomaterialia,* vol. 10, no. 6, pp. 2341-2353, 2014.

[33] J. L. Bredas and G. B. Street, "Polarons, bipolarons, and solitons in conducting polymers," *Accounts of chemical research,* vol. 18, no. 10, pp. 309-315, 1985.

[34] A. G. MacDiarmid, R. Mammone, R. Kaner, and L. Porter, "The concept of 'doping'of conducting polymers: The role of reduction potentials," *Philosophical Transactions of the Royal Society of London. Series A, Mathematical and Physical Sciences,* vol. 314, no. 1528, pp. 3-15, 1985.

[35] F. Jonas, G. Heywang, W. Schmidtberg, J. Heinze, and M. Dietrich, "Polythiophenes, process for their preparation and their use," ed: Google Patents, 1990.

[36] S. Nie, Z. Li, Y. Yao, and Y. Jin, "Progress in synthesis of conductive polymer poly (3, 4-ethylenedioxythiophene)," *Frontiers in Chemistry,* vol. 9, p. 803509, 2021.

[37] U. Lang, E. Müller, N. Naujoks, and J. Dual, "Microscopical investigations of PEDOT: PSS thin films," *Advanced Functional Materials,* vol. 19, no. 8, pp. 1215-1220, 2009.

[38] Y. Wen and J. Xu, "Scientific importance of water-processable PEDOT–PSS and preparation, challenge and new application in sensors of its film electrode: a review," *Journal of Polymer Science Part A: Polymer Chemistry,* vol. 55, no. 7, pp. 1121-1150, 2017.

[39] Z. Ahmad, A. W. Azman, Y. F. Buys, and N. Sarifuddin, "Mechanisms for doped PEDOT: PSS electrical conductivity improvement," *Materials Advances,* vol. 2, no. 22, pp. 7118-7138, 2021.

[40] D. C. Martin and G. G. Malliaras, "Interfacing electronic and ionic charge transport in bioelectronics," *ChemElectroChem,* vol. 3, no. 5, pp. 686-688, 2016.

[41] S. T. Keene, V. Gueskine, M. Berggren, G. G. Malliaras, K. Tybrandt, and I. Zozoulenko, "Exploiting mixed conducting polymers in organic and bioelectronic devices," *Physical Chemistry Chemical Physics,* vol. 24, no. 32, pp. 19144-19163, 2022.

[42] E. Stavrinidou *et al.*, "Direct measurement of ion mobility in a conducting polymer," *Advanced Materials,* vol. 25, no. 32, pp. 4488-4493, 2013.

[43] Y. Li, X. Zhou, B. Sarkar, N. Gagnon-Lafrenais, and F. Cicoira, "Recent Progress on Self-Healable Conducting Polymers," *Advanced Materials,* vol. 34, no. 24, p. 2108932, 2022.

[44] A. D. Godwin, "28 - Plasticizers," in *Applied Plastics Engineering Handbook*, M. Kutz Ed. Oxford: William Andrew Publishing, 2011, pp. 487-501.

[45] L. V. Kayser and D. J. Lipomi, "Stretchable conductive polymers and composites based on PEDOT and PEDOT: PSS," *Advanced Materials*, vol. 31, no. 10, p. 1806133, 2019.

[46] H. He and J. Ouyang, "Enhancements in the mechanical stretchability and thermoelectric properties of PEDOT: PSS for flexible electronics applications," *Accounts of Materials Research*, vol. 1, no. 2, pp. 146-157, 2020.

[47] X. Gao *et al.*, "Bioelectronic Applications of Intrinsically Conductive Polymers," *Advanced Electronic Materials*, p. 2300082, 2023.

[48] H. He *et al.*, "Biocompatible conductive polymers with high conductivity and high stretchability," *ACS applied materials & interfaces*, vol. 11, no. 29, pp. 26185-26193, 2019.

[49] Y. Li *et al.*, "Autonomic Self-Healing of PEDOT: PSS Achieved Via Polyethylene Glycol Addition," *Advanced Functional Materials*, vol. 30, no. 30, p. 2002853, 2020.

[50] H. He, L. Zhang, S. Yue, S. Yu, J. Wei, and J. Ouyang, "Enhancement in the mechanical stretchability of PEDOT: PSS films by compounds of multiple hydroxyl groups for their application as transparent stretchable conductors," *Macromolecules*, vol. 54, no. 3, pp. 1234-1242, 2021.

[51] M. Vosgueritchian, D. J. Lipomi, and Z. Bao, "Highly conductive and transparent PEDOT: PSS films with a fluorosurfactant for stretchable and flexible transparent electrodes," *Advanced functional materials*, vol. 22, no. 2, pp. 421-428, 2012.

[52] B. Marchiori, R. Delattre, S. Hannah, S. Blayac, and M. Ramuz, "Laser-patterned metallic interconnections for all stretchable organic electrochemical transistors," *Scientific reports*, vol. 8, no. 1, p. 8477, 2018.

[53] J. Y. Oh, S. Kim, H. K. Baik, and U. Jeong, "Conducting polymer dough for deformable electronics," *Advanced Materials*, vol. 28, no. 22, pp. 4455-4461, 2016.

[54] Y. Wang *et al.*, "A highly stretchable, transparent, and conductive polymer," *Science advances*, vol. 3, no. 3, p. e1602076, 2017.

[55] H. Shi, C. Liu, Q. Jiang, and J. Xu, "Effective approaches to improve the electrical conductivity of PEDOT: PSS: a review," *Advanced Electronic Materials*, vol. 1, no. 4, p. 1500017, 2015.

[56] D. Alemu, H.-Y. Wei, K.-C. Ho, and C.-W. Chu, "Highly conductive PEDOT: PSS electrode by simple film treatment with methanol for ITO-free polymer solar cells," *Energy & environmental science*, vol. 5, no. 11, pp. 9662-9671, 2012.

[57] M. Z. Seyedin, J. M. Razal, P. C. Innis, and G. G. Wallace, "Strain-responsive polyurethane/PEDOT: PSS elastomeric composite fibers with high electrical conductivity," *Advanced Functional Materials*, vol. 24, no. 20, pp. 2957-2966, 2014.

[58] L. Zhang *et al.*, "Fully organic compliant dry electrodes self-adhesive to skin for long-term motion-robust epidermal biopotential monitoring," *Nature communications*, vol. 11, no. 1, pp. 1-13, 2020.

[59] M. Abbasipour, P. Kateb, F. Cicoira, and D. Pasini, "Stretchable kirigami-inspired conductive polymers for strain sensors applications," *Flexible and Printed Electronics*, 2023.

[60] R. Luo, H. Li, B. Du, S. Zhou, and Y. Zhu, "A simple strategy for high stretchable, flexible and conductive polymer films based on PEDOT: PSS-PDMS blends," *Organic Electronics*, vol. 76, p. 105451, 2020.

[61] H. Jo'Elen *et al.*, "Flexible and stretchable printed conducting polymer devices for electrodermal activity measurements," *Flexible and Printed Electronics*, 2022.

[62] M. Azimi, C.-h. Kim, J. Fan, and F. Cicoira, "Effect of Ionic Conductivity of Electrolyte on Printed Planar and Vertical Organic Electrochemical Transistors," *Faraday Discussions*, 10.1039/D3FD00065F 2023, doi: 10.1039/D3FD00065F.

[63] C.-H. Kim, M. Azimi, J. Fan, H. Nagarajan, M. Wang, and F. Cicoira, "All-printed and stretchable organic electrochemical transistors using a hydrogel electrolyte," *Nanoscale*, 10.1039/D2NR06731E vol. 15, no. 7, pp. 3263-3272, 2023, doi: 10.1039/D2NR06731E.

[64] R. Das, X. He, and K. Ghaffarzadeh, "Flexible, printed and organic electronics 2019–2029: forecasts, players & opportunities," *IDTechEx. com*, 2018.

[65] E. Bihar *et al.*, "Fully printed electrodes on stretchable textiles for long-term electrophysiology," *Advanced Materials Technologies*, vol. 2, no. 4, p. 1600251, 2017.

[66] Y. Khan, A. Thielens, S. Muin, J. Ting, C. Baumbauer, and A. C. Arias, "A new frontier of printed electronics: flexible hybrid electronics," *Advanced Materials*, vol. 32, no. 15, p. 1905279, 2020.

[67] Y. Khan, A. E. Ostfeld, C. M. Lochner, A. Pierre, and A. C. Arias, "Monitoring of vital signs with flexible and wearable medical devices," *Advanced materials*, vol. 28, no. 22, pp. 4373-4395, 2016.

[68] M. A. Leenen, V. Arning, H. Thiem, J. Steiger, and R. Anselmann, "Printable electronics: Flexibility for the future," *physica status solidi (a)*, vol. 206, no. 4, pp. 588-597, 2009.

[69] L. D. Garma, L. M. Ferrari, P. Scognamiglio, F. Greco, and F. Santoro, "Inkjet-printed PEDOT:PSS multi-electrode arrays for low-cost in vitro electrophysiology," *Lab on a Chip*, 10.1039/C9LC00636B vol. 19, no. 22, pp. 3776-3786, 2019, doi: 10.1039/C9LC00636B.

[70] Y. D. Kim and J. Hone, "Screen printing of 2D semiconductors," *Nature*, vol. 544, no. 7649, pp. 167-168, 2017.

[71] C. Kapnopoulos *et al.*, "Fully gravure printed organic photovoltaic modules: A straightforward process with a high potential for large scale production," *Solar Energy Materials and Solar Cells*, vol. 144, pp. 724-731, 2016.

[72] S. Liu *et al.*, "Self-Healing, Robust, and Stretchable Electrode by Direct Printing on Dynamic Polyurea Surface at Slightly Elevated Temperature," *Advanced Functional Materials,* vol. 31, no. 26, p. 2102225, 2021, doi: https://doi.org/10.1002/adfm.202102225.

[73] B. Seong, H. Lee, J. Lee, L. Lin, H.-S. Jang, and D. Byun, "Biomimetic, flexible, and self-healable printed silver electrode by spontaneous self-layering phenomenon of a gelatin scaffold," *ACS applied materials & interfaces,* vol. 10, no. 30, pp. 25666-25672, 2018.

[74] F. Ye, M. Li, D. Ke, L. Wang, and Y. Lu, "Ultrafast Self-Healing and Injectable Conductive Hydrogel for Strain and Pressure Sensors," *Advanced Materials Technologies,* vol. 4, no. 9, p. 1900346, 2019.

[75] X. Su *et al.*, "A Highly Conducting Polymer for Self-Healable, Printable, and Stretchable Organic Electrochemical Transistor Arrays and Near Hysteresis-Free Soft Tactile Sensors," *Advanced Materials,* vol. 34, no. 19, p. 2200682, 2022.

[76] G. E. Bergey, R. D. Squires, and W. C. Sipple, "Electrocardiogram recording with pasteless electrodes," *IEEE Transactions on Biomedical Engineering,* no. 3, pp. 206-211, 1971.

[77] Y.-H. Chen *et al.*, "Soft, comfortable polymer dry electrodes for high quality ECG and EEG recording," *Sensors,* vol. 14, no. 12, pp. 23758-23780, 2014.

[78] H.-C. Jung *et al.*, "CNT/PDMS composite flexible dry electrodesfor long-term ECG monitoring," *IEEE Transactions on Biomedical Engineering,* vol. 59, no. 5, pp. 1472-1479, 2012.

[79] L.-F. Wang, J.-Q. Liu, B. Yang, and C.-S. Yang, "PDMS-based low cost flexible dry electrode for long-term EEG measurement," *IEEE Sensors Journal,* vol. 12, no. 9, pp. 2898-2904, 2012.

[80] D. Pani, A. Achilli, and A. Bonfiglio, "Survey on textile electrode technologies for electrocardiographic (ECG) monitoring, from metal wires to polymers," *Advanced Materials Technologies,* vol. 3, no. 10, p. 1800008, 2018.

[81] P. A. Haddad, A. Servati, S. Soltanian, F. Ko, and P. Servati, "Breathable dry silver/silver chloride electronic textile electrodes for electrodermal activity monitoring," *Biosensors,* vol. 8, no. 3, p. 79, 2018.

[82] S. Takamatsu, T. Lonjaret, D. Crisp, J.-M. Badier, G. G. Malliaras, and E. Ismailova, "Direct patterning of organic conductors on knitted textiles for long-term electrocardiography," *Scientific reports,* vol. 5, no. 1, p. 15003, 2015.

[83] D. Pani, A. Dessì, J. F. Saenz-Cogollo, G. Barabino, B. Fraboni, and A. Bonfiglio, "Fully textile, PEDOT: PSS based electrodes for wearable ECG monitoring systems," *IEEE Transactions on Biomedical Engineering,* vol. 63, no. 3, pp. 540-549, 2015.

[84] K. Zhang *et al.*, "Skin Conformal and Antibacterial PPy-Leather Electrode for ECG Monitoring," *Advanced Electronic Materials,* vol. 6, no. 8, p. 2000259, 2020.

[85] F. Stauffer *et al.*, "Skin conformal polymer electrodes for clinical ECG and EEG recordings," *Advanced healthcare materials,* vol. 7, no. 7, p. 1700994, 2018.

[86] H. F. Posada-Quintero, R. Rood, Y. Noh, K. Burnham, J. Pennace, and K. H. Chon, "Dry carbon/salt adhesive electrodes for recording electrodermal activity," *Sensors and Actuators A: Physical,* vol. 257, pp. 84-91, 2017.

[87] S. K. Sinha *et al.*, "Integrated dry poly (3, 4-ethylenedioxythiophene): polystyrene sulfonate electrodes on finished textiles for continuous and simultaneous monitoring of electrocardiogram, electromyogram and electrodermal activity," *Flexible and Printed Electronics,* vol. 5, no. 3, p. 035009, 2020.

[88] A. Aguzin *et al.*, "Gelatin and tannic acid based iongels for muscle activity recording and stimulation electrodes," *ACS Biomaterials Science & Engineering,* vol. 8, no. 6, pp. 2598-2609, 2022.

[89] G. Li *et al.*, "Highly conducting and stretchable double-network hydrogel for soft bioelectronics," *Advanced Materials,* vol. 34, no. 15, p. 2200261, 2022.

[90] L. You *et al.*, "Flexible porous Gelatin/Polypyrrole/Reduction graphene oxide organohydrogel for wearable electronics," *Journal of Colloid and Interface Science,* vol. 625, pp. 197-209, 2022.

[91] G. Shen *et al.*, "A novel flexible hydrogel electrode with a strong moisturizing ability for long-term EEG recording," *Journal of Neural Engineering,* vol. 18, no. 6, p. 066047, 2021.

[92] C. Boehler, Z. Aqrawe, and M. Asplund, "Applications of PEDOT in bioelectronic medicine," *Bioelectronics in Medicine,* vol. 2, no. 2, pp. 89-99, 2019.

[93] N. Rossetti *et al.*, "Poly (3, 4-ethylenedioxythiophene)(PEDOT) Coatings for High-Quality Electromyography Recording," *ACS Applied Bio Materials,* vol. 2, no. 11, pp. 5154-5163, 2019.

[94] K. Polachan, B. Chatterjee, S. Weigand, and S. Sen, "Human Body–Electrode Interfaces for Wide-Frequency Sensing and Communication: A Review," *Nanomaterials,* vol. 11, no. 8, p. 2152, 2021. [Online]. Available: https://www.mdpi.com/2079-4991/11/8/2152.

[95] E. McAdams, "Bioelectrodes," *Encyclopedia of Medical Devices and Instrumentation,* 2006.

[96] P. Biesheuvel, S. Porada, and J. Dykstra, "The difference between Faradaic and non-Faradaic electrode processes," *arXiv preprint arXiv:1809.02930,* 2018.

[97] V. Button and V. Button, "Electrodes for biopotential recording and tissue stimulation," *Principles of Measurement and Transduction of Biomedical Variables; Academic Press: Oxford, UK,* pp. 25-76, 2015.

[98] M. O'Sullivan, A. Temko, A. Bocchino, C. O'Mahony, G. Boylan, and E. Popovici, "Analysis of a low-cost EEG monitoring system and dry electrodes toward clinical use in the neonatal ICU," *Sensors,* vol. 19, no. 11, p. 2637, 2019.

[99] A. F. de Bengy, J. Lamartine, D. Sigaudo-Roussel, and B. Fromy, "Newborn and elderly skin: two fragile skins at higher risk of pressure injury," *Biological Reviews,* vol. 97, no. 3, pp. 874-895, 2022.

[100] X. Guo and A. Facchetti, "The journey of conducting polymers from discovery to application," *Nature Materials,* vol. 19, no. 9, pp. 922-928, 2020.

[101] L. A. Schachner and R. C. Hansen, *Pediatric dermatology*. Elsevier Health Sciences, 2011.

[102] P. M. Elias, "Stratum corneum defensive functions: an integrated view," *Journal of Investigative Dermatology,* vol. 125, no. 2, pp. 183-200, 2005.

[103] D. Garrod and M. Chidgey, "Desmosome structure, composition and function," *Biochimica et Biophysica Acta (BBA)-Biomembranes,* vol. 1778, no. 3, pp. 572-587, 2008.

[104] C. Lund, "Medical adhesives in the NICU," *Newborn and Infant Nursing Reviews,* vol. 14, no. 4, pp. 160-165, 2014.

[105] M. L. W. Erin F. Mathes. "Skin of the Premature Infant." https://clinicalgate.com/skin-of-the-premature-infant/#bib63 (accessed.

[106] J. M. Karp and R. Langer, "Dry solution to a sticky problem," *Nature,* vol. 477, no. 7362, pp. 42-43, 2011.

[107] C. H. Lund, L. B. Nonato, J. M. Kuller, L. S. Franck, C. Cullander, and D. K. Durand, "Disruption of barrier function in neonatal skin associated with adhesive removal," *The Journal of pediatrics,* vol. 131, no. 3, pp. 367-372, 1997.

[108] M. K. Kwak, H. E. Jeong, and K. Y. Suh, "Rational design and enhanced biocompatibility of a dry adhesive medical skin patch," *Advanced Materials,* vol. 23, no. 34, pp. 3949-3953, 2011.

[109] I. Hwang *et al.*, "Multifunctional smart skin adhesive patches for advanced health care," *Advanced healthcare materials,* vol. 7, no. 15, p. 1800275, 2018.

[110] Voltera. "https://www.voltera.io/product/specs." (accessed.

[111] A. R. Spencer *et al.*, "Bioprinting of a cell-laden conductive hydrogel composite," *ACS applied materials & interfaces,* vol. 11, no. 34, pp. 30518-30533, 2019.

[112] S. Zhang *et al.*, "Room-temperature-formed PEDOT: PSS hydrogels enable injectable, soft, and healable organic bioelectronics," *Advanced Materials,* vol. 32, no. 1, p. 1904752, 2020.

[113] N. Rossetti, H. Jo'Elen, P. Kateb, and F. Cicoira, "Neural and electromyography PEDOT electrodes for invasive stimulation and recording," *Journal of Materials Chemistry C,* vol. 9, no. 23, pp. 7243-7263, 2021.

[114] P. Tan *et al.*, "Solution-processable, soft, self-adhesive, and conductive polymer composites for soft electronics," *Nature communications,* vol. 13, no. 1, pp. 1-12, 2022.

[115] Y. Li *et al.*, "Tailoring the Self-Healing Properties of Conducting Polymer Films," *Macromolecular Bioscience,* vol. 20, no. 11, p. 2000146, 2020.

[116] S. Zhang and F. Cicoira, "Water-Enabled Healing of Conducting Polymer Films," *Advanced Materials,* vol. 29, no. 40, p. 1703098, 2017.

[117] P. J. Taroni *et al.*, "Toward stretchable self-powered sensors based on the thermoelectric response of PEDOT: PSS/polyurethane blends," *Advanced Functional Materials,* vol. 28, no. 15, p. 1704285, 2018.

[118] J. Joseph, R. Patel, A. Wenham, and J. Smith, "Biomedical applications of polyurethane materials and coatings," *Transactions of the IMF,* vol. 96, no. 3, pp. 121-129, 2018.

[119] E. J. Shin and S. M. Choi, "Advances in waterborne polyurethane-based biomaterials for biomedical applications," *Novel biomaterials for regenerative medicine,* pp. 251-283, 2018.

[120] B. R. Barrioni, S. M. de Carvalho, R. L. Oréfice, A. A. R. de Oliveira, and M. de Magalhães Pereira, "Synthesis and characterization of biodegradable polyurethane films based on HDI with hydrolyzable crosslinked bonds and a homogeneous structure for biomedical applications," *Materials Science and Engineering: C,* vol. 52, pp. 22-30, 2015.

[121] A. International, *ASTM D882-12, Standard test method for tensile properties of thin plastic sheeting*. ASTM International, 2012.

[122] M. AST, "Standard Test Method for 90 Degree Peel Resistance of Adhesives," *ASTM International, West Conshohocken, PA, Standard,* no. D6862-11, 2016.

[123] D. Makowski *et al.*, "NeuroKit2: A Python toolbox for neurophysiological signal processing," *Behavior research methods,* pp. 1-8, 2021.

[124] C. Carreiras, A. P. Alves, A. Lourenço, F. Canento, H. Silva, and A. Fred, "BioSPPy: Biosignal Processing in Python. 2015," *URL https://github. com/PIA-Group/BioSPPy,* 2018.

[125] J. Kim, Y. Hwang, S. Jeong, S. Y. Lee, Y. Choi, and S. Jung, "An elastomer for epidermal electronics with adjustable adhesion force and stretchability obtained via a reverse-micelle-induced process," *Journal of Materials Chemistry C,* vol. 6, no. 9, pp. 2210-2215, 2018.

[126] M. Waring, S. Bielfeldt, and M. Brandt, "Skin adhesion properties of three dressings used for acute wounds," *Wounds UK,* vol. 5, no. 3, pp. 22-31, 2009.

[127] L. Wang, J. Wang, C. Fan, T. Xu, and X. Zhang, "Skin-like hydrogel-elastomer based electrochemical device for comfortable wearable biofluid monitoring," *Chemical Engineering Journal,* p. 140609, 2022.

[128] A. Kalra, A. Lowe, and A. Al-Jumaily, "Mechanical behaviour of skin: a review," *J. Mater. Sci. Eng,* vol. 5, no. 4, p. 1000254, 2016.

[129] S. Timpanaro, M. Kemerink, F. Touwslager, M. De Kok, and S. Schrader, "Morphology and conductivity of PEDOT/PSS films studied by scanning–tunneling microscopy," *Chemical Physics Letters,* vol. 394, no. 4-6, pp. 339-343, 2004.

[130] T. Wang, Y. Qi, J. Xu, X. Hu, and P. Chen, "Effects of poly (ethylene glycol) on electrical conductivity of poly (3, 4-ethylenedioxythiophene)–poly (styrenesulfonic acid) film," *Applied surface science*, vol. 250, no. 1-4, pp. 188-194, 2005.

[131] Y. Li, X. Zhou, B. Sarkar, N. Gagnon-Lafrenais, and F. Cicoira, "Recent progresses on Self-healable Conducting Polymers," *Advanced materials*, p. e2108932, 2022.

[132] Q. Wei, M. Mukaida, W. Ding, and T. Ishida, "Humidity control in a closed system utilizing conducting polymers," *RSC advances*, vol. 8, no. 23, pp. 12540-12546, 2018.

[133] F. Roig, E. Dantras, J. Dandurand, and C. Lacabanne, "Influence of hydrogen bonds on glass transition and dielectric relaxations of cellulose," *Journal of Physics D: Applied Physics*, vol. 44, no. 4, p. 045403, 2011.

[134] I. 10993-5, "Biological evaluation of medical devices—Part 5: Tests for in vitro cytotoxicity," *IOS, Switzerland*, 2009.

[135] E. Bihar, T. Roberts, M. Saadaoui, T. Hervé, J. B. De Graaf, and G. G. Malliaras, "Inkjet-printed PEDOT: PSS electrodes on paper for electrocardiography," *Advanced healthcare materials*, vol. 6, no. 6, p. 1601167, 2017.

[136] S. K. Sinha *et al.*, "Screen-printed PEDOT: PSS electrodes on commercial finished textiles for electrocardiography," *ACS applied materials & interfaces*, vol. 9, no. 43, pp. 37524-37528, 2017.

[137] G. Fredi *et al.*, "Bioinspired Polydopamine Coating as an Adhesion Enhancer Between Paraffin Microcapsules and an Epoxy Matrix," *ACS Omega*, vol. 5, no. 31, pp. 19639-19653, 2020/08/11 2020, doi: 10.1021/acsomega.0c02271.

[138] D. Hauser, D. Septiadi, J. Turner, A. Petri-Fink, and B. Rothen-Rutishauser, "From bioinspired glue to medicine: polydopamine as a biomedical material," *Materials*, vol. 13, no. 7, p. 1730, 2020.

[139] M. A. Gwak, B. M. Hong, J. M. Seok, S. A. Park, and W. H. Park, "Effect of tannic acid on the mechanical and adhesive properties of catechol-modified hyaluronic acid hydrogels," *International Journal of Biological Macromolecules*, vol. 191, pp. 699-705, 2021.

[140] H. Jafari *et al.*, "Tannic acid: a versatile polyphenol for design of biomedical hydrogels," *Journal of Materials Chemistry B*, vol. 10, no. 31, pp. 5873-5912, 2022.

APPENDIX A ARTICLE 1: SUPPLEMENTARY INFORMATION

Supplementary material

Printable, adhesive and self-healing dry epidermal electrodes based on PEDOT:PSS and polyurethane diol

Pierre Kateb[1], Jiaxin Fan[1], Jinsil Kim[1], Xin Zhou[1], Gregory A. Lodygensky[2] and Fabio Cicoira[1*]

[1]*Polytechnique Montréal, 2500 Chemin de Polytechnique, Montreal, Quebec H3T 1J4, Canada*

[2]*Sainte-Justine University Hospital Research Center, 520 Rue Bélanger, Montreal, Quebec H1T 1C9, Canada*

*Corresponding author's email: fabio.cicoira@polymtl.ca

Figure S 5. Photos of PEDOT:PSS films with 5% PUD, 5% PEG and 5% sorbitol (Sorb) in glass vials a) before adding water and, b) approximately 5 seconds, and c) 1 h immersed in water.

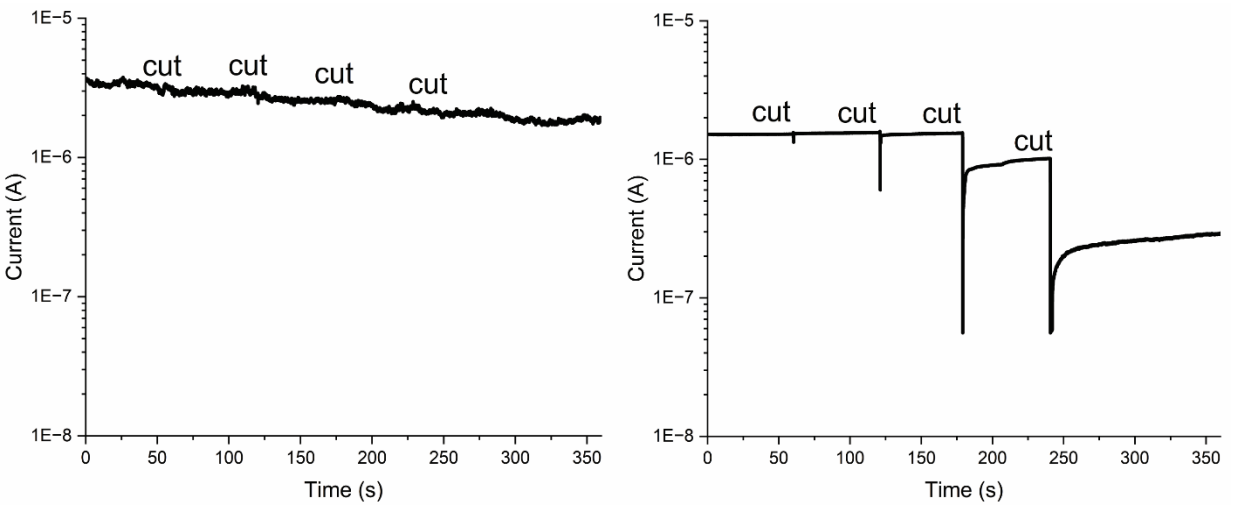

Figure S 6. Current change of free-standing PEDOT:PSS films with a) 5% PEG and b) 5% sorbitol when cut, showing their electrical self-healing behaviors.

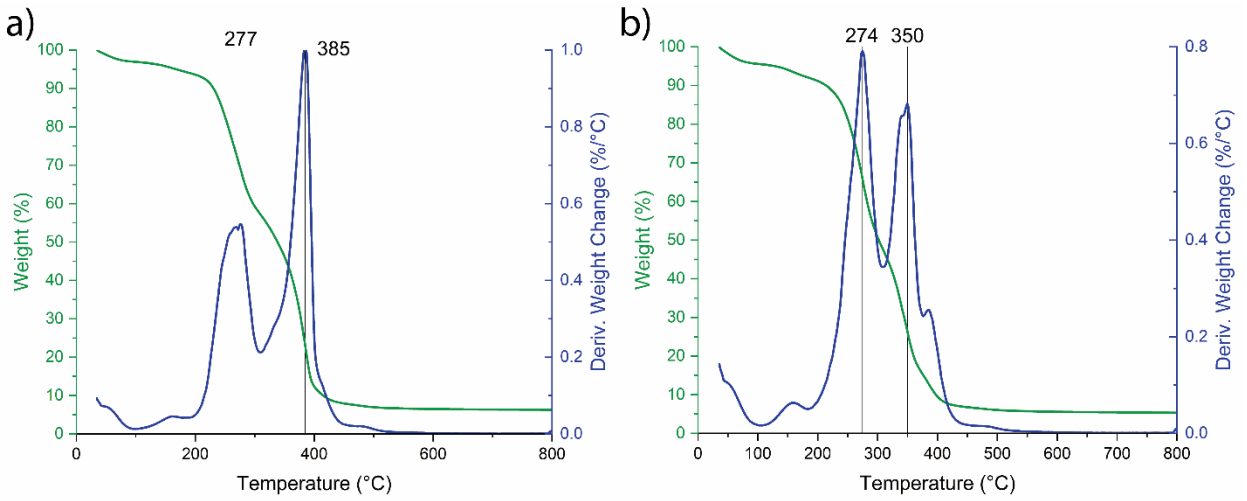

Figure S 7. Thermogravimetric analysis curves of PEDOT:PSS based films with a) 2% sorbitol and 5% PUD and b) 2% PEG and 5% PUD.

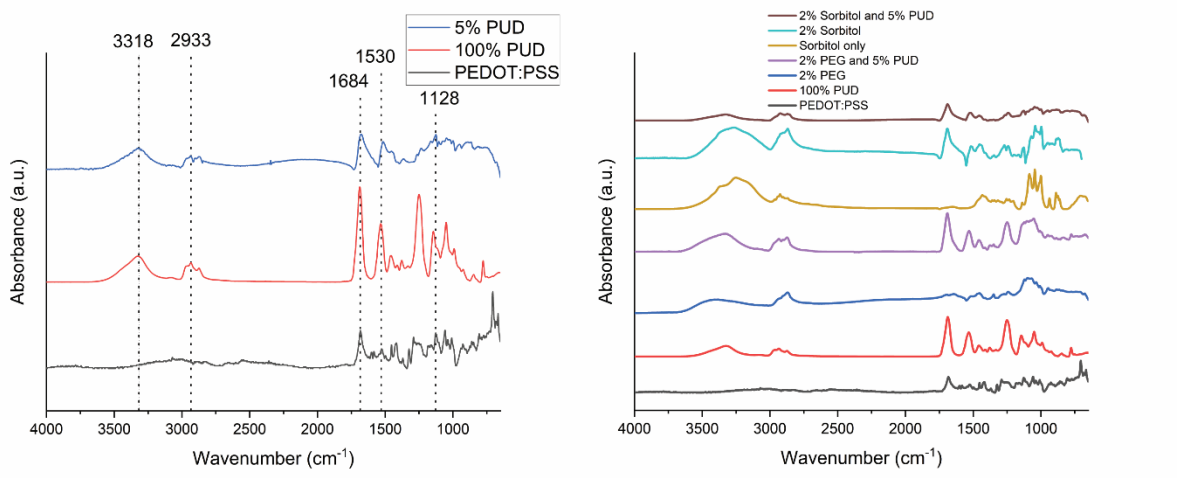

Figure S 8. Fourier transform infrared spectrophotometry (FTIR) of a) pristine PEDOT:PSS, pristine PUD, and PEDOT:PSS with 5% PUD and b) thin films for PEDOT:PSS with different additives.

Table S 1. Thickness of different free-standing PEDOT:PSS based films. Data were obtained from measurements of three different samples (n = 3) and are reported as mean ± standard deviation.

PEDOT:PSS mixture	Thickness (µm)
Pristine PEDOT:PSS	11 ± 1
2% PUD	25 ± 2
5% PUD	38 ± 3
10% PUD	60 ± 8
2% PEG	14 ± 2
5% PEG	40 ± 3
2% PEG and 2% PUD	37 ± 3
2%PEG and 5% PUD	44 ± 1
2% Sorbitol	18 ± 2
5% Sorbitol	49 ± 3
2% Sorbitol and 2% PUD	51 ± 2
2% Sorbitol and 5% PUD	67 ± 6

Table S 2**.** Adhesion on glass and on fake skin of PEDOT:PSS films based on different formulations. Data (n = 3) is reported as mean ± standard deviation.

PEDOT:PSS mixtures	Adhesion (N/cm)	
	On glass	On fake skin
Pristine PEDOT:PSS	N/A	N/A
2% PUD	N/A	N/A
5% PUD	0.066 ± 0.011	0.032 ± 0.001
10% PUD	0.051 ± 0.005	0.028 ± 0.005
2% PEG	0.006 ± 0.001	N/A
5% PEG	0.005 ± 0.001	N/A
2% PEG and 2% PUD	0.005 ± 0.001	0.003 ± 0.001
2% PEG and 5% PUD	0.006 ± 0.001	0.005 ± 0.001
2% Sorbitol	0.012 ± 0.002	N/A
5% Sorbitol	0.242 ± 0.063	0.011 ± 0.001
2% Sorbitol and 2% PUD	0.062 ± 0.003	0.029 ± 0.003
2% Sorbitol and 5% PUD	0.052 ± 0.008	0.034 ± 0.004
Ecoflex	0.233 ± 0.022	0.045 ± 0.002

Table S 3**.** Mechanical properties, including Young's Modulus and elongation at break, and electrical conductivity of PEDOT:PSS films based on different formulations. Data (n = 3) is reported as mean ± standard deviation.

PEDOT:PSS mixtures	Young's Modulus (MPa)	Elongation (%)	Conductivity (S/cm)
Pristine PEDOT:PSS	2396 ± 121	5.1 ± 0.2	0.5 ± 0.1
2% PUD	151 ± 8	15.4 ± 0.9	21.6 ± 4.3
5% PUD	15.1 ± 1.8	33.0 ± 1.8	32.3 ± 5.0
10% PUD	5.8 ± 0.8	41.0 ± 2.2	2.5 ± 0.3
2% PEG	56.0 ± 2.6	17.3 ± 0.9	312.6 ± 46.4
5% PEG	10.0 ± 1.6	16.4 ± 1.9	113.6 ± 11.7
2% PEG and 2% PUD	10.7 ± 1.3	21.5 ± 1.4	92.8 ± 5.3
2%PEG and 5% PUD	8.2 ± 1.5	29.0 ± 1.9	99.4 ± 14.3
2% Sorbitol	15.0 ± 2.9	29.9 ± 0.4	7.9 ± 2.4
5% Sorbitol	7.3 ± 1.9	62.4 ± 2.8	1.3 ± 0.1
2% Sorbitol and 2% PUD	15.3 ± 1.6	32.0 ± 2.1	13.4 ± 3.2
2% Sorbitol and 5% PUD	6.0 ± 0.6	40.3 ± 2.4	14.0 ± 0.8

Table S 4**.** Conductivities for sorbitol/PEDOT:PSS films annealed at high temperature. Data (n=3) is reported as mean ± standard deviation.

PEDOT:PSS mixtures	Conductivity (S/cm)
2% Sorbitol	273.9 ± 8.8
5% Sorbitol	48.8 ± 3.4
2% Sorbitol and 2% PUD	110.9 ± 3.6
2% Sorbitol and 5% PUD	29.5 ± 3.7

Table S 5**.** Young's Modulus and elongation at break for PEDOT:PSS films containing 5% PUD, 5% PEG and 5% sorbitol after storage in ambient conditions for one week. Data (n = 3) is reported as mean ± standard deviation.

PEDOT:PSS mixtures	Young's Modulus (MPa)	Elongation (%)
5% PUD	23.7 ± 4.0	22.5 ± 2.1
5% PEG	11.8 ± 0.5	15.1 ± 1.6
5% Sorbitol	209.7 ± 22.1	6.8 ± 1.2

APPENDIX B CONTRIBUTIONS TO PAPERS

- Zhou, X., **Kateb, P.**, Miquet-Westphal, F., Lodygensky, G.A., Cicoira, F. (2023). Soft, conductive and anti-freezing conducting polymer organohydrogels. Advanced Sensor Research.
- Petrossian, G., **Kateb, P.**, Miquet-Westphal, F., & Cicoira, F. (2023). Advances in Electrode Materials for Scalp, Forehead, and Ear EEG: A Mini-Review. ACS Applied Bio Materials. doi:10.1021/acsabm.3c00322
- Abbasipour, M., **Kateb, P.**, Cicoira, F., & Pasini, D. (2023). Stretchable kirigami-inspired conductive polymers for strain sensors applications. Flexible and Printed Electronics.
- Hagler, J., Kim, C., **Kateb, P.**, Yeu, J., Gagnon-Lafrenais, N., Gee, E., Audry, S., & Cicoira, F. (2022). Flexible and stretchable printed conducting polymer devices for electrodermal activity measurements. Flexible and Printed Electronics, 7(1), 014008.
- Rossetti, N., Hagler, J., **Kateb, P**., & Cicoira, F. (2021). Neural and electromyography PEDOT electrodes for invasive stimulation and recording. Journal of Materials Chemistry C, 9(23), 7243-7263.

Submitted

- **Kateb, P.**, Fan, J., Kim, J., Zhou, X., Lodygensky, G.A., Cicoira, F. (2023). Printable, adhesive and self-healing dry epidermal electrodes using PEDOT:PSS and polyurethane diol. Flexible and Printed Electronics
- Zhou, X., **Kateb, P.**, Kim, J., Lodygensky, G.A., Cicoira, F. (2023). Stretchable, Soft, Highly Adhesive, and Self-healing Conductive Polymer Films for Healthcare Monitoring. Chemical Engineering Journal.
- Wang, M., Kim, J., Miquet-Westphal, F., Zhou, X., **Kateb, P.**, Fan, J., Cicoira, F. (2023). Self-healable PEDOT-based film, hydrogel and OECT device for bioelectronics. Materials Matter.